AN MRI COMPATIBLE BAND GAP DEPENDENT FIBER OPTIC TEMPERATURE SENSOR

by

Ahmet Deniz

B.S., Electrical and Electronics Engineering, Boğaziçi University, 2015

Submitted to the Institute for Graduate Studies in
Science and Engineering in partial fulfillment of
the requirements for the degree of
Master of Science

Graduate Program in Electrical and Electronics Engineering
Boğaziçi University

2018

ACKNOWLEDGEMENTS

I would first like to express my deepest appreciation to my thesis advisor Prof. Arda Deniz Yalçınkaya for his support, guidance and patience. I was always welcomed by Prof. Arda Deniz Yalçınkaya whenever i had a question about my study. He always managed to steer me to the right direction, although he had busy schedule.

I would also like to express my special thanks to the rest of my thesis committee: Assist. Prof. Onur Ferhanoğlu and Assist. Prof. İlke Ercan.

I am deeply greateful to my friends, Mehmet Batman, Hakan Canöz, Berk As, Amin Soltani, Osman Deniz, Ömer Karasu, for their supports through this study.

Finally, I must express my strong feelings about my family for supporting me under any conditions. I am sincerely greateful to my parents Mehmet Emin Deniz, Şevkiye Deniz, my brother Halit Deniz and my sister Latife Deniz.

Thanks to TÜBİTAK 1001 Project 116E814.

ABSTRACT

AN MRI COMPATIBLE BAND GAP DEPENDENT FIBER OPTIC TEMPERATURE SENSOR

Fiber optic sensors (FOTSs) have been a research topic over two decades. Many sensor types were developed in different schemes. Among many other parameters like pressure, location, PH level detection..etc, which can be measured by fiber optic sensors, temperature sensor is one of the most important, widely used and studied sensor in many fields such as medical applications like minimally invasive surgeries, In-Situ Thermal Remediation (ISTR) and oil and gas production and transportation.

The objective of this thesis is to research transmittance and reflectance dependence with the temperature in order to help developing a fiber optic microsystem temperature sensor based on the concept of the band gap energy of a gallium arsenide (GaAs) to give information to the non-invasive medical instruments under the magnetic resonance imaging (MRI). Fiber optic sensor has immunity to electromagnetic (EM) interference which is one of the best reasons to use it under the MRI.

Among other semiconductors, GaAs is one of the most convenient material due to the its direct band gap . Direct band gap provides direct transitions of electrons from valence band to conduction band due to valence band and conduction band are in the same crystal momentum. So, electrons does not require an extra energy to conservation of their momentum, this provides good absorption and emission of light. Based on the properties of the GaAs, temperature changes can be monitored with a insignificant delay and error.

Temperature sensing is based on the reflectance, transmittance and absorbance changes in the semiconductor with respect to temperature. Incident light at carefully

determined wavelength will be reflected and transmitted with the different intensities and correspondingly different powers at every different temperature. Light transmission and reflection through the GaAs crystal is also wavelength dependent. In this thesis, transmitted light power will be measured by photodetector under different temperatures.

ÖZET

BAND GAP DEĞİŞİMİNE BAĞLI FİBER OPTİK SICAKLIK SENSÖRÜ

Fiber optik sıcaklık sensörleri yirmi yılı aşkın bir süredir araştırma konusudur. Bir çok sensör çeşidi çok farklı yollarla üretilmektedir. Basınç, konum, PH değeri ölçümü gibi sensörler tarafından ölçülebilen bir çok parametrenin yanında, sıcaklık sensörü bir çok alanda en önemli, en çok kullanılan ve en çok araştırılan sensörlerden biridir. Grişimsel olmayan medikal opearsyonlar, sıcaklıkla toprağın iyileştirilmesi, petrol ve gaz üretimi ve dağıtımı alanları bu alanlardan bazılarıdır.

Bu tezin amacı, MRI cihazı altında müdahalesiz medikal enstrümanlara bilgi sağlayan, galyum arsenit (GaAs) yarı iletkeninin bant aralığı enerjisini baz alan fiber optik mikrosistem sensörlerin geliştirilmesine yardımcı olması amacıyla band gap'in sıcaklıkla değişmesine bağlı geçirgenlik değişimlerini gözlemlemektir.

Diğer yarı iletkenler arasında, GaAs'in direkt bant aralığı GaAs'i en uygun maddelerden biri haline getirir. Direkt bant aralığı, elektronların ekstra bir enerjiye duymadan valans bandından iletken banda geçmesine olanak sağlar. GaAs'in özelliklerine bağlı olarak, sıcaklık değişimleri çok küçük bir gecikme ve hata ile izlenebilir.

Sıcaklık algılama, sıcaklığa bağlı olarak değişen yarı iletkenin yansıtma, geçirgenlik ve soğurma özelliklerindeki değişimleri baz alır. Belirlenen dalga boyunda gelen ışık, her farklı sıcaklıkta farklı yoğunluk ve güçte yansır ve iletilir. Işığın GaAs kristal üzerinden yansıması ve iletilmesi aynı zamanda dalga boyuna bağlıdır. Bu tezde ışığın iletilen ışığın gücü, farklı sıcaklıklarda bir foto dedektör yardımıyla ölçülecektir.

TABLE OF CONTENTS

LIST OF FIGURES

LIST OF SYMBOLS

B_I	Incident magnetic field
B_{0i}	Amplitude of the incident magnetic field
B_R	Reflected magnetic field
B_{0r}	Amplitude of the reflected magnetic field
B_T	Transmitted magnetic field
B_{0t}	Amplitude of the transmitted magnetic field
C	Celcius
c	Speed of the light in vacuum
E_c	Conduction band energy
E_g	Band gap energy
$E_g(T)$	Band gap energy with respect to temperature
$E_g(0)$	Band gap energy at room temperature
E_I	Incident electric field
E_{0i}	Amplitude of the incident electric field
E_{0r}	Amplitude of the reflected electric field
E_T	Transmitted electric field
E_{0t}	Amplitude of the transmitted electric field
E_v	Valence band energy
eV	Electron volt
h	Planck constant
I	Intensity
I_0	Intensity of the incident light
I_R	Intensity of the reflected light
I_T	Intensity of the transmitted light
$\hat{i}$	Unit vector of the polarization of the electric field
$\hat{j}$	Unit vector of the polarization of the magnetic field
$\vec{k}$	Propagation vector
$\hat{k}$	Direction of the propagation vector

l	Thickness
n	Index of refraction
$\frac{\partial n}{\partial T}$	Index of refraction change per degree
p	Momentum
R	Reflectance
r	Reflection coefficient
T	Transmittance
v	Speed of the light in a medium
α	Absorption coefficient
ϵ_0	Permittivity in vacuum
Θ_i	Angle between incident light and normal of the surface
Θ_r	Angle between reflected light and normal of the surface
Θ_t	Angle between transmitted light and normal of the surface
λ_c	Cut-off wavelength
μm	Micrometer

LIST OF ACRONYMS/ABBREVIATIONS

ISTR	In-Situ Thermal Remediation
EM	Electromagnetic
FOTS	Fiber Optic Temperature Sensor
MR	Magnetic Resonance
MRI	Magnetic Resonance Imaging
GaAs	Gallium Arsenide
Ga	Gallium
As	Arsenide
MW	Microwave
MWA	Microwave Ablation
RF	Radio Frequency
RFA	Radio Frequency Ablation
HIFU	High Intensity Focused Ultrasound
LA	Laser Ablation
CB	Conduction Band
VB	Valence Band
NIR	Near Infrared
LED	Laser Dide
PCB	Printed Circuit Board
DC	Direct Current
SSP	Single Side Polished
DSP	Double Side Polished

1. INTRODUCTION

Temperature measurement is crucial in variety of research fields such as medical areas [1], oil and gas industries [2] and ecological applications like In-Situ Thermal Remediation (ISTR) [3] in today's world. Besides optical temperature sensors, there can be found other kinds of temperature sensors like thermistors [4]and thermocouples [5]. But these sensors have some disadvantages when compared to the optical sensors [6] due to their sizes and lack of immunity to external disturbances like electromagnetic (EM) field [7].

Temperature sensing devices can be found in many different forms depending on their application fields. A simple mercury based thermometer is enough to measure the weather, but it is not viable for measurement of the temperature of internal organs. A thermistor can measure the desired object but under the electrical or magnetic field, it can not be enough due to its high sensitivity to electrical or magnetic field [8]. Thermistor shows the temperature according to the current through the temperature dependent resistor whose resistance depends on the temperature. Under an EM field, current value can change due to electromagnetic induction [9].

At this point, fiber optic temperature sensors play a crucial role due to their small size and passive characteristics [10] to the harsh environments.

Reflection mode operation based fiber optic sensors generally use the data over the reflected light from the sensor at the end of the fiber cable tip. Reflected light can be in the same fiber cable or another fiber cable can be used as the path of the reflected light.

Two of the most common methods for fiber optic temperature sensing are demonstrated in the figure 1.1.

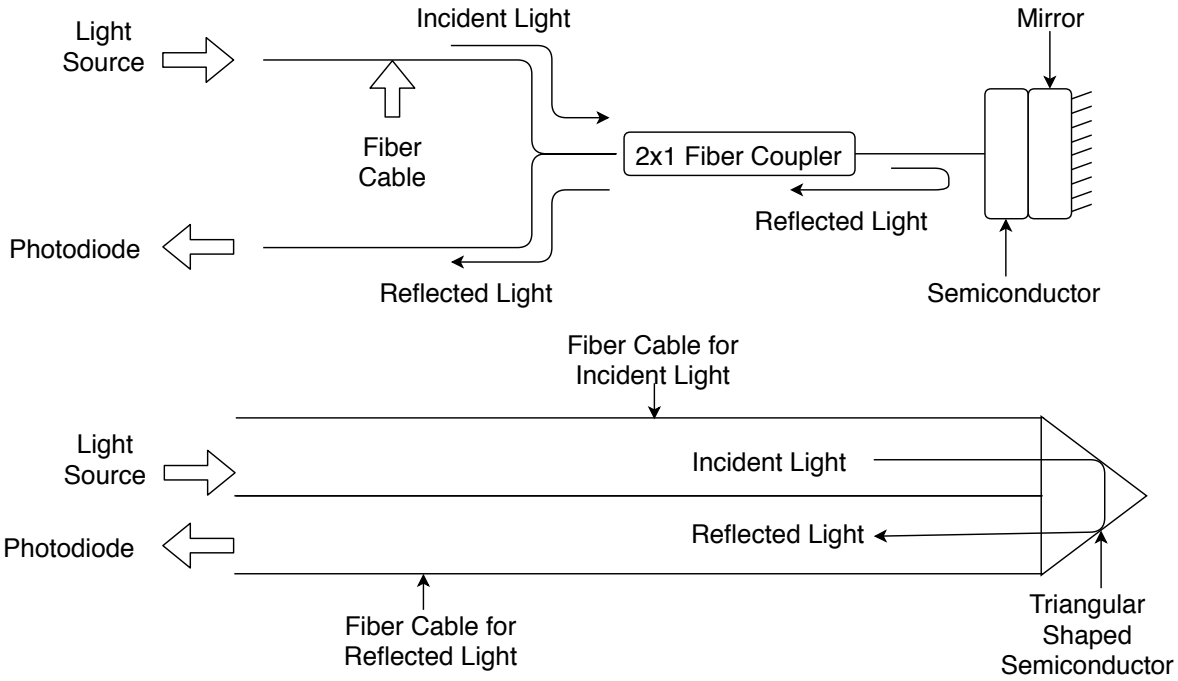

Figure 1.1. Two different methods for detecting reflected light.

The method given on the upper side of the figure 1.1 is the dominant method for commercial usage of fiber optic temperature sensors. As can bee seen in the upper side figure, light comes from the light source goes through the fiber cable and interacts with sensor which is a semiconductor wafer. Some of the light gets absorbed by the semiconductor and some of the light reflects back. Due to the dielectric mirror, transmission does not occur. The following method has a triangular semiconductor to get total reflection. When the incoming light is bigger than the critical angle in the triangular semiconductor, it reflects back totally [11].

There are two important points in the upper method. To increase the intensity of the reflected light, a dielectric mirror [12] deposition can be done to the other side of the incident light. It reflects back the light that should be transmitted. In more detail, the light goes into the semiconductor, reflects back from the mirror and again goes into the semiconductor. That means absorption occurs two times or it can be thought of as light goes and penetrates semiconductor with doubled thickness. The advantage of this method can be say in a simple mathematical sentence, if there is no mirror behind

the semiconductor material, reflected light would be:

$$R_{\mathbf{nm}} = 1 - T - A \tag{1.1}$$

where R_{nm} is reflection with no mirror, T refers to transmission and A is the absorption. As the mirror placed, returned light becomes:

$$R_{\mathbf{m}} = 1 - 2A \tag{1.2}$$

R_m refers to reflection with the dielectric mirror deposited. It can be said that returned light also includes transmitted light.

Another key is fiber coupler which has a key role for illuminated light and reflected light to be in one fiber cable. It splits the light in desired ratios. In the following figure, dielectric mirror placement and 2x1 fiber coupler can be seen in figure 1.1.

Experiments can have different ways to measure other than commercial industry models, modified light can be observed as a reflection or transmission and setups can be done in many ways. In section 2.3 Three different ways are described and shown. Experimental setups are of course has disadvantages compare to professional factory-made FOTSs. Main disadvantage is the calibration of the tools to align laser source, wafer and photodiode. Disadvantages is told shortly in the section 2.3.

The aim of this thesis is designing a fiber optical temperature sensor (FOTS) experiment to guide the further experiments for making commercial fiber optic temperature sensors. Some important expectations from the FOTSs are accuracy as low as $\pm 0.1°C$, fast response time as short as 10 ms and immunity to EM interference so that it can be use especially in the field of medical industry. Besides these features, small dimensions of the optical sensors [6] allow many usage area in medical technology. For example, in the field of interventional cardiology and oncology, temperature

feedback is highly important for operations like laser ablation catheter [13] to avoid injuries in patient's cardiovascular system. These operations can be performed under MRI [14] and needs fast response and immunity to the EM interferences [15]. Fiber optic temperature sensors (FOTSs) [16] provides these features with a beam of light in a fiber optic cable with a semiconductor at the tip of the fiber.

Basic mechanism of this sensor is measuring the temperature by detecting the intensity of the reflected light from the semiconductor material using photo-detector. Temperature variations affect the optical absorption edge [17] of the semiconductor. As the temperature increases, distance between atoms increases due to vibration energy of atoms. And outermost electrons take place in valence band. And between the adjacent atoms, an periodic potential occurs [18] which is a potential energy when electrons are pass by other atoms or ions. There is an inverse relation between the inter-atomic distance and electric potential [19].

Optical absorption edge wavelength [20] depends on the band gap energy of the semiconductor materials. Optical absorption edge wavelength is also called cut-off optical wavelength. Cut-off wavelength is the wavelength that semiconductor material starts to transmit the incident light. This specific wavelength and temperature have direct proportion. In other words, as the temperature increases, cut-off wavelength increases and vice versa. Cut-off wavelength of semiconductor can be found from the formula 1.3.

$$\lambda_c = \frac{hc}{E_g}\,(\mu m) \tag{1.3}$$

where E_g is the band gap energy of semiconductor, λ_c is cutoff wavelength, h is planck constant and c is the speed of light in vacuum. Among many other methods, band gap absorption is the preferred method in this thesis due to the aim of the thesis which is measuring low temperatures such as the temperature values inside the cardiovascular system. When the semiconductor material gets its transmission spectra gets to higher wavelengths, in other words, it transmits to photons with lower energy and opposite situation occur when the temperature decreases due to its band gap characteristics. In

the thesis, appropriate semiconductor is chosen as Gallium Arsenide (GaAs) due to its convenient features.

GaAs (Gallium Arsenide) is a well known semiconductor material which compounds gallium(Ga) from column III and arsenic(As) from column V. GaAs has a direct band gap which is a very good and desirable feature for optical sensor. GaAs semiconductor is the material that will be fitted on the tip of the fiber optic cable. FOTS depend on the absorption and transmission of the GaAs crystal. As the temperature increases, band gap of a GaAs crystal [21] decreases and it allows the transmission of the longer wavelengths. Longer wavelength means less photon energy detected by photo-detector.

In this thesis, instead of using different wavelengths, only one wavelength is selected near the cut-off wavelength. That is because of choosing one wavelength has low cost. Transmission and reflection values of the specific wavelength is observed.

1.1. Background and Applications

Communication with light through optical fibers concept was first researched by Dr. K. C. Kao and G. A. Hockham in 1966 [22]. This modern low lost optical fiber cables were introduced after the first functional laser designed by Theodore H. Maiman in 1960 [23]. After these two significant inventions, in the beginning of the 1970s [24], scientists started to focus on sensor technologies via fiber optic cables. Since then so many sensor types such as pressure, temperature, chemical sensing, humidity..etc have been developed and it's still a growing research area [25].

First studies have done for the military aircrafts and rockets [26]. That is because aircrafts and rockets have harsh environmental conditions when they fly and they need to more sensitive sensors to overcome critical computations.

After almost two decades from the fibre concept, FOTSs were spread to other areas scuh as medical applications [24] and oil industry [27]. It started to take it place

in the market. But until the 1990s, fibre sensors had obstacles compared to other sensor types [28]. First of all, fibre sensors had quite small market comparing to other sensors. That is because the usage area of the fibre sensors have not been increased then. And cost was an another obstacle to improve the fibre sensor technology [28].

In time, fibre sensor were started to be needed because of new technologies and applications were developed for specific requirements. Magnetic Resonance Imaging (MRI) is one of the examples that widely known. During the minimally invasive operations under MRI, some feedbacks like temperature and pressure [29] are necessary for accuracy of the operation. And the need for small devices and passive sensors are another reasons to increase the demand for the fibre sensors because electrical transducers respond to magnetic field under MRI and their functions are degraded [30].

After the 1990s, improvements have been accelerated and cost of the fiber optic technologies and sensors related to that have been decreased significantly. This provided an opportunity to studies to further developments. Different kind of fibre optic sensors such as pressure [31], temperature [32] and location sensors [33] have took their places in the market [28].

As mentioned briefly earlier, FOTSs have significant place among all other sensor types which detects variety of parameters such as pressure [31] , radiation [34] , acceleration [35], location [33], etc. Along with the fast progress in FOTS area, application fields of the fiber optic sensors are also expanding.

1.1.1. Medical Applications

Recent developments prove that fiber optic sensors are quite useful in medical applications. Accuracy and fast response in harsh environments is two of the desired characteristics in the medical area.

As the technological developments proceed, main objective of the medical operations becomes to perform less invasive processes and avoid open surgeries [36]. Medical

advancements provides radio frequency (RF) ablations [37] or surgical operation with miniaturized tools to avoid circumstances that mentioned. During the advanced operations, temperature tracking has a vital role [32]. Fiber optic temperature sensors' small size may vary from 100 microns to a few microns. FOTSs' small size allows physicians to track temperature in real time in such operations.

Accurate and instantaneous tracking of temperature is important in operations like laser therapy [13], cryotherapy [38], microwave (MW) [39] or RF based treatments [37] because of the prevent overheating to the targeted site.

FOTSs can be used to measure the temperature of the body parts such as the temperature inside the blood vessels or internal organs. That is because of the small size of the FOTS is quite suitable for vessels. Minimally invasive surgical operations needs to miniaturized tools as expected, FOTSs can be highly miniaturized and become useful in these kind of operations [40].

Here is some medical operations that need temperature tracking:

- High intensity focused ultrasound (HIFU) [41] can penetrate the soft tissue and gives direct heating to targeted tissue. Targeted tissue absorbs ultrasonic energy and gets thermally heated. Some of the HIFU operations need MRI guidance. Thermal tracking is done by the fiber optic sensors in HIFU operations [42].
- Laser ablation (LA) [13] is an another method to thermally heat the tumor. It contacts the tumor site and it needs to be temperature tracking with the help of the FOTSs.
- Microwave (MW) therapy [39] or MW ablation (MWA) sends EM waves to water molecules, due to water molecules are polar, this EM waves creates frictional energy as a result of electrical charge on the water molecules. Lung and liver cancer treatments can be done by the help of the MW ablation and it needs to be done under MR imaging to locate the lesion. As predicted, temperature monitoring is an inevitable in the MW ablation process and FOTSs plays the role in it.

- RF ablation (RFA) [37] is another mehtod for tissue heating by creating electric field lines through the body of the patient.

Laser ablation (LA) [13], RF [37] and MW ablation [39] and HIFU [41] treatments are some techniques that can used in cancer treatments by burning the targeted tissues by ablation or hyperthermia. Different techniques have roles in different areas like interventional cardiology, vascular diseases, cancer treatments. These techniques need a fast temperature feedback as told before to protect healthy cells from the electrical, magnetic or EM field and also exact timing is important for destroying diseased tissue.

Fast response to the temperature variations, minimal structure and immunity to EM fields are three main reasons for using FOTS in medical area [40] and additional features are described as benefits of the FOTSs in the section 1.2.

In addition to temperature measurement, fiber optic sensors can detect many other physical or chemical parameters. For physical parameters, some of examples are pressure [31], localization [33] and strain sensing [43]. Some examples for chemical sensing are detecting PH level of the blood [43], determining oxygen or carbon-dioxide level in the blood [44]. There are variety of parameters that need to be tracked in surgical operations and fiber sensors manage to track them and these parameters have crucial role during the surgical operation.

Immunity to electrical, magnetic and EM field important feature. Electromagnetic field induces current in conventional electrical sensors and disrupts the functionality and causes malfunctions [45]. Magnetic resonance imaging is indispensable in variety of invasive or non invasive operations. Immunity of FOTSs provides lots of benefits to track necessary parameters under the MRI. Like all other fiber optic sensor types, fiber optic temperature sensor is irresponsive to the magnetic field which is desirable for surgical operations which performed under the MRI.

MRI working principle and physics [46] behind it should be mentioned because of it is a essential device in today's medical area. It is an imaging technique that shows

3D images of the soft tissues in high resolution with the ability to show differences in physiological changes. MRI is founded and demonstrated in the year 1946 by Purcell [47] and F. Bloch [48] seperately. To imaging the targeted area of the body, one should be positioned inside the MRI scanner and strong magnets of the MRI device create strong and uniform magnetic field around the targeted area. Although magnetic field shows differences in different systems, most of the clinical MRI systems uses either 1.5 T or 3 T which is about four orders of magnitude higher than the earth's magnetic field [46].

Under such a large magnetic field, only passive elements like fiber optic sensors can track the vital parameters in the targeted tissue [10].

For emphasizing the importance of fiber optic temperature monitoring, following example will be helpful. For intervention on the selected tumor, avoiding the damage the healthy tissue during the thermal treatment is the aim of the surgical procedure.In order to this, first, tumor position and its physical properties such as its geometry is determined accurately by the surgeon [49]. Thermal treatment is started to apply to ablate the tumor site with the help of real time temperature monitoring. Real time temperature monitoring provides the surgeon to decide thermal exposure time on tumor site. Temperature and time of exposure are the main parameters for thermally ablating the tumor cells without harm the healthy tissues [40]. This can be best done by the fiber optic temperature monitoring systems.

As an a little detailed example for usage area of the FOTSs in the Radio-frequency Thermal Ablation (RFA) [50] in liver, lung and other tissues is mentioned as follows; this procedure is resembles to previous definitions, RFA's [50] aim is the treat small sized tumors basically in liver, lung, kidney. RFA creates temperature field at the target tumor site. It needs temperature monitoring as the given example before.

1.1.2. Ecological Applications

Besides medical industry, FOTSs can be used in the decontamination of the toxic fields which contaminated by oil. For this procedure, heating the soil with the help of radio frequencies is used. FOTSs are used to monitor the temperature during the clearing process [51].

1.1.3. Oil and Gas Industry

Oil industries search for oil and gas kilometers below the earth crust. Temperature measurement has an important role in determining the locations of the oil and gas. These locations have temperature over 100°C. At such temperatures, electrical temperature sensors have potential to explode inside the oil and gas reserves [27]. Due to the passive nature of FOTSs, they are preferable to traditional electrical temperature sensors.

Medical applications of FOTSs is especially emphasized because of it is the main objective of this thesis.

1.2. Advantages of the FOTSs

There are lots of advantages of fiber optic temperature sensors such as immunity to EM field and small size [10], flexibility and sensitivity. FOTSs advantages has to be proven to take market share in the temperature sensor market place. Advantages of the FOTSs mentioned in three subsections.

1.2.1. Electromagnetic and Radio Frequency Interference Immunity

Fiber optic cables are generally manufactured from two types of material according to which range they needed for; glass [52] or plastic [53]. Almost all fiber optic cables and sensors have passive elements which means there are no electrical circuit on them [10]. This feature gives fiber optic sensors a very good advantage. Due to

the fiber cables communicate with light instead of electrons [54], they do not react to electrical, magnetic, electromagnetic or radio frequency disturbances [10]. Immunity brings another advantage apart from the other sensor types. Other electrical circuit based sensor types need to be protected from the external disturbances which means that they need to be shielded [55] to become unresponsive to the electric, magnetic or electromagnetic effects because these fields induces an electrical current which affects the measurement accuracy [8] Shielding process [55] enlarge their sizes. But fiber optic sensors do not have to be shielded and this brings the advantage of small size that is desirable for many medical applications.

1.2.2. Small Size, Flexibility and Safety

Fiber optic sensors can be quite small in size. Their diameter can range from a couple of microns to a few millimeters [56] depending on the application requirements. In a complicated surgery, a lot of surgical instruments can be needed and lots of instruments mean increasing the surgical operation area which is not a desired condition. Miniaturized instruments help to reduce the surgical operation area. Another demand for small sized fiber optic sensors is sometimes operations can be highly sensitive that millimeters becomes important during the operations such as placing a stent into blood vessels [57]. During these kind of operations, monitoring the patient's conditions with the conventional sensors insufficient because of their improper sizes. FOTSs have vital roles due to their small sizes.

Flexibility and Safety are among the other important advantages of the FOTSs [58]. Fiber optic cables are highly flexible which is a good feature for so many medical applications. Monitoring curled parts of the body is achieved by this flexibility.

For safety issues, with no doubt, fiber optic sensors are the most trustable sensor type due to their intrinsic characteristics which does not include active electrical circuitry that can be affected by EM fields. For example, oil companies use fiber optic cables to monitor the temperature of the oil wells [2, 27] for safety issues. In other words, fiber optic cable does not carry field induced current which may pose hazardous

explosions [54].

Another thing for safety of FOTSs is that they do not need to be shielded due to external disturbances not only for EM fields but also humidity or extreme temperatures [59]. They can be used in long term monitoring where ever they desired.

1.2.3. Accuracy and stability

High sensitivity in FOTSs needs a professional calibration with high quality equipments. A well tuned fiber optic sensor may have the accuracy of $\pm 0.1^{\circ}$C [32].

Stability is another important factor for FOTSs. Harsh environments such as humidity or high temperatures can harm the electrical based temperature sensors [10]. But FOTSs have durable character that can be stable for a long time during monitoring environments that other sensors can not withstand.

1.3. Contributions of the Thesis

Some contributions of the thesis to the next studies and literature presented as follows:

- This thesis deal with the miniaturized fiber optic temperature sensor which based on the band gap energy of the GaAs. This thesis deals with the determination of the change of in the transmission and reflection with 3 different experiments. Reflection measurement method is described as follows; illuminated light from the laser source reflects back from the semiconductor material GaAs and goes to the photodiode detector. Transmission analysis can be done by placing the photodiode the back of the semiconductor and try to avoid external noises such as ambient light.
- Another contribution of the thesis to the next studies is selecting the right semiconductor. In other words, specifications are important for the chosen semiconductors. In this thesis, experiments are done in difficult situations because of the

chosen gallium arsenide. This difficulties are due to lack of information in the literature about gallium arsenide physical condition properties such as polishing and misleading the company that GaAs wafer bought. Explanations about GaAs will show the way to the other new studies that which parameters should be taking into consideration when buying gallium arsenide wafer.

1.4. Organization of the Thesis

Organization of the thesis is as follows. In chapter 2, gallium arsenide pyhsical and optical properties are introduced. GaAs characteristics are given and it's band structure is shown. After that, theoritical methods are explained to understand the relationhip between temperature and band gap for semiconductors. Some calculations are made to use them when they are necessary. Then, setups of the experiment are shown in the figures. Setups of experiments are explained in detail and tools that used in the setups are introduced.

In chapter 3, results from the setups are displayed. Reflected and transmitted power versus temperature graphs are presented. Linearity between temperature and transmission and reflection in measured temperatures are indicated. Analyzing the results are made. Absorption coefficient versus temperature linearity is shown. Reasons behind low transmission are explained.

In chapter 4, comments about experimental results are made. Future work advices are given.

2. DESIGN AND METHODS

In this chapter, firstly, we will mentione the physics of the GaAs semiconductor material. Advantages of using GaAs are reviewed. After that, temperature measurement mechanism is defined. Formulations related to light transmission through the direct band gap semiconductors are given. Then, components for the experiment are presented. Finally, experimental setup is demonstrated explanatorily with the photos of the experiment.

2.1. Physical and Optical Properties of GaAs

Some properties of the semiconductors needs to be known in order to progress in designing and understanding of the fiber optic temperature sensor. We will briefly explain some basic fundamentals that based on the GaAs semiconductor. Detailed information about semiconductor physics can be found in the semiconductor devices, physics and technology textbook by Simon Sze and Ming-Kwei Lee [60] which is this thesis's reference for some brief information of the semiconductor physics.

Gallium arsenide (GaAs) consists of gallium (Ga) from column III and arsenic (As) from column V, which makes GaAs a III-V compound. GaAs has a direct band gap and it's a crystalline material which has a Zincblende structure. It's colour is grey and it's melting point is 1238°C [61]. GaAs can not find in nature. GaAs first created by the Goldschmidt [62] in 1920's.

Electrons can only be in discrete energy levels in solid materials [63]. Band gap can be defined as restricted area to the electrons. In other words, bad gap is the difference in energy between bottom of the conduction band and top of the valence band which are allowed energy levels for the electrons. Band gap energy E_g is the width of the forbidden energy gap between conduction band energy E_c and valence band energy E_v which is E_c - E_v [64, 65]. Energy band structure of GaAs can be seen in Figure 2.1.

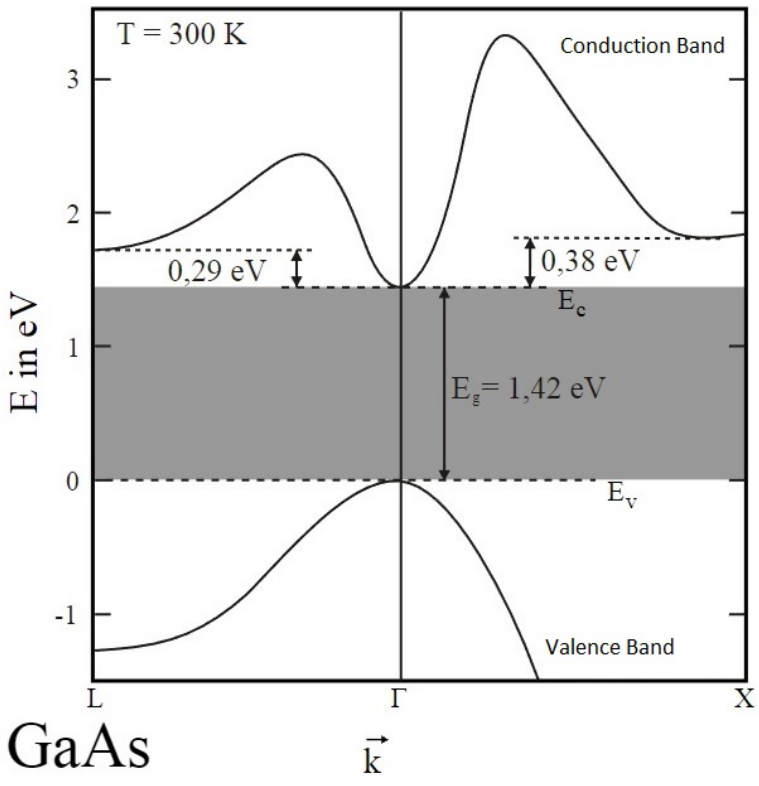

Figure 2.1. Energy band structure of GaAs [66].

Momentum is zero at Γ-valley in figure 2.1. As we can see from the figure 2.1, minimum of the conduction band and the maximum of the valence band take place at the momentum p =0 which is what we want for this thesis because otherwise we would need a phonon that adds momentum to electron to get the conduction band. In other words, transition of electrons from valence band to the conduction band needs no momentum. This makes GaAs direct band gap semiconductor.

2.2. Theoritical Measurement Method

Light interaction with the semiconductor material is a wavelength dependent phenomenon. Illuminated light can be absorbed, transmitted and reflected. When the light emitted from the laser source to the semiconductor material, photons are absorbed substantially if the incident light energy is equal or greater than the band gap energy of the semiconductor material [60]. That means, reflected light intensity decreases proportional to the absorption.

When the incident photon energy is greater than band gap energy E_g, photon absorption increases rapidly and this point can be referred as cut-off wavelength or transition wavelenght. We can find the cutoff wavelength from the formula below

$$\lambda_c = \frac{hc}{E_g} \tag{2.1}$$

where λ_c is cutoff wavelength, h is planck constant and c is the speed of light in vacuum. hc equals to 1.24 eV-μm. Rearrangement of equation 2.1 gives us:

$$\lambda_c = \frac{1.24}{E_g}\,(\mu m) \tag{2.2}$$

We can have an information about transition (cutoff) wavelength through the GaAs at the room temperature. Using the band gap energy of GaAs as 1.42 eV, we can calculate the necessary wavelength to illuminate to the semiconductor is $\frac{1.24}{1.42}\,(\mu m) = 0.873\,(\mu m)$ which is in the near infrared region of the spectrum.

When the temperature rises, band gap energy decreases. The increase in temperature causes the atoms to vibrate more. This increased vibration causes the rise in the interatomic distance. This leads to an decrease in potential energy [18]. Varshni [67] have succeeded to show the relation between band gap and temperature in equation 2.5.

Interatomic distance and electron energy relationship can be seen in figure 2.2

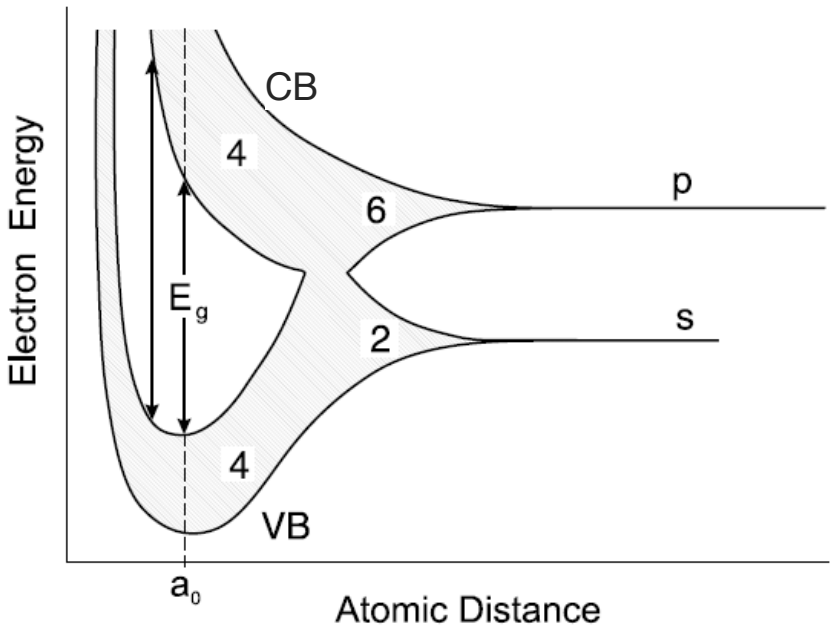

Figure 2.2. Electron Energy vs Atomic Distance [19]

As seen from the figure 2.2, band gap width decreases with respect to increasing interatomic distance [68]. CB represents the conduction band and VB represents the valence band. Band gap eventually disappears as we go through the right of the figure 2.2.

As can be seen from Varshni equation 2.5, if temperature increases, the band gap decreases, exciting the electrons at the valence band becomes easier and less energy is required to it, followed by increase in absorption. That means cut off wavelength shifts to the longer wavelengths which do not have enough energy to excite the electrons

at valence band. We can see the figure 2.3 as an example for shifting the longer wavelengths with the increasing temperature.

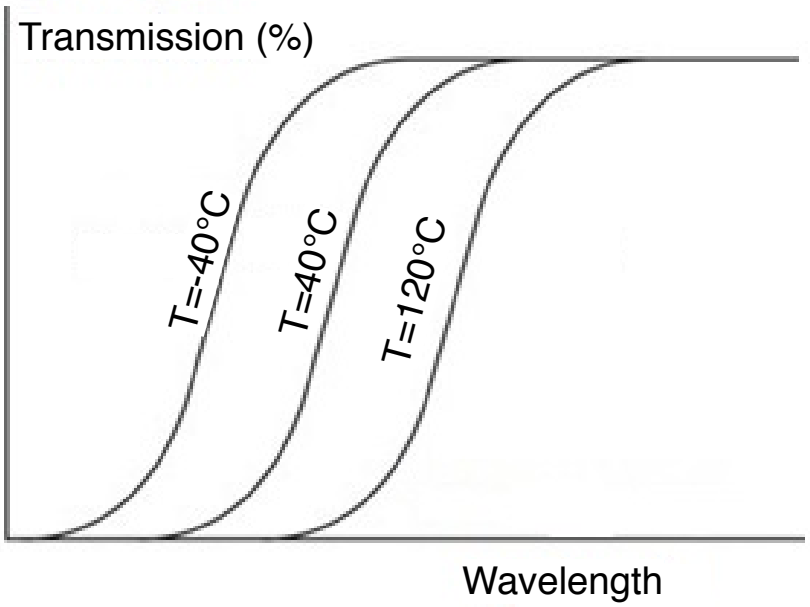

Figure 2.3. Transmission vs wavelength with 3 different temperatures.

We can interpret the figure 2.3 in a different way. We can see that cut-off wavelength shifts toward the right with increasing temperature. This shift of cut-off wavelength means that required energy for transmission decreases. Instead of detecting the cut-off wavelength points on the transmission graph, we can observe changes in the light by just it's energy.

Absorption coefficient a can be defined as the fraction of the absorbed photons with per unit distance which has unit of cm^{-1}. This thesis focus on the wavelengths around the cutoff wavelength. So, we can use the simplified version of the Urbach rule [69] from the formula below

$$a = A\sqrt{(h\nu - E_g(T))} \tag{2.3}$$

where a is the absorption coefficient which is temperature T dependent, $h\nu$ is the photon energy, $E_g(T)$ is the band gap energy with respect to temperature and A is a constant for semiconductor (GaAs) material.

To obtain equations for transmission we can assume that reflection occurs both sides equally with a normally incident light. Taking into account the internal reflections, we can see the intensity of the transmitted light in its last form in the figure 2.5. İnternal reflection will become negligible due to the absorption through the way of propagated light which is formulated and showed in the figure 2.5. After first reflection, light propagates through the thickness l and attenuated by e^{-al} [70]. Attenuation of the light can be seen in figure 2.4. This attenuation occurs every time light reflects back inside the medium.

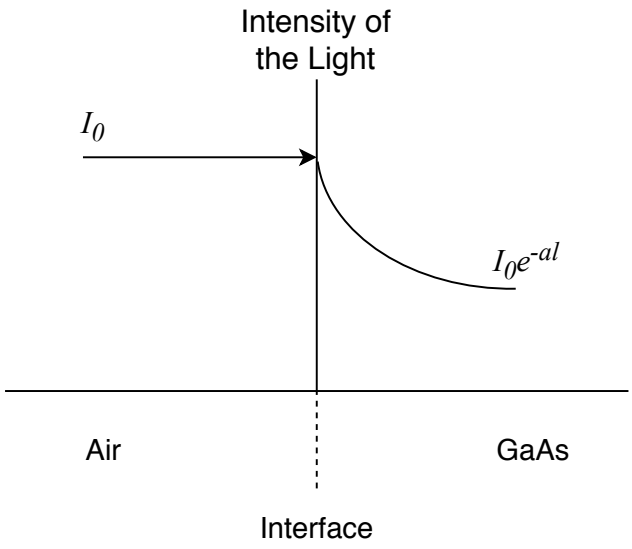

Figure 2.4. Attenuation of the Light.

If we sum all the transmitted lights and divide it to the incoming light I_0, Transmittance becomes;

$$T = (1-R)^2 e^{-al}[1 + R^2e^{-2} + ...R^{2n-1}e^{2n}] = \frac{(1-R)^2e^{-al}}{1-R^2e^{-2al}} \tag{2.4}$$

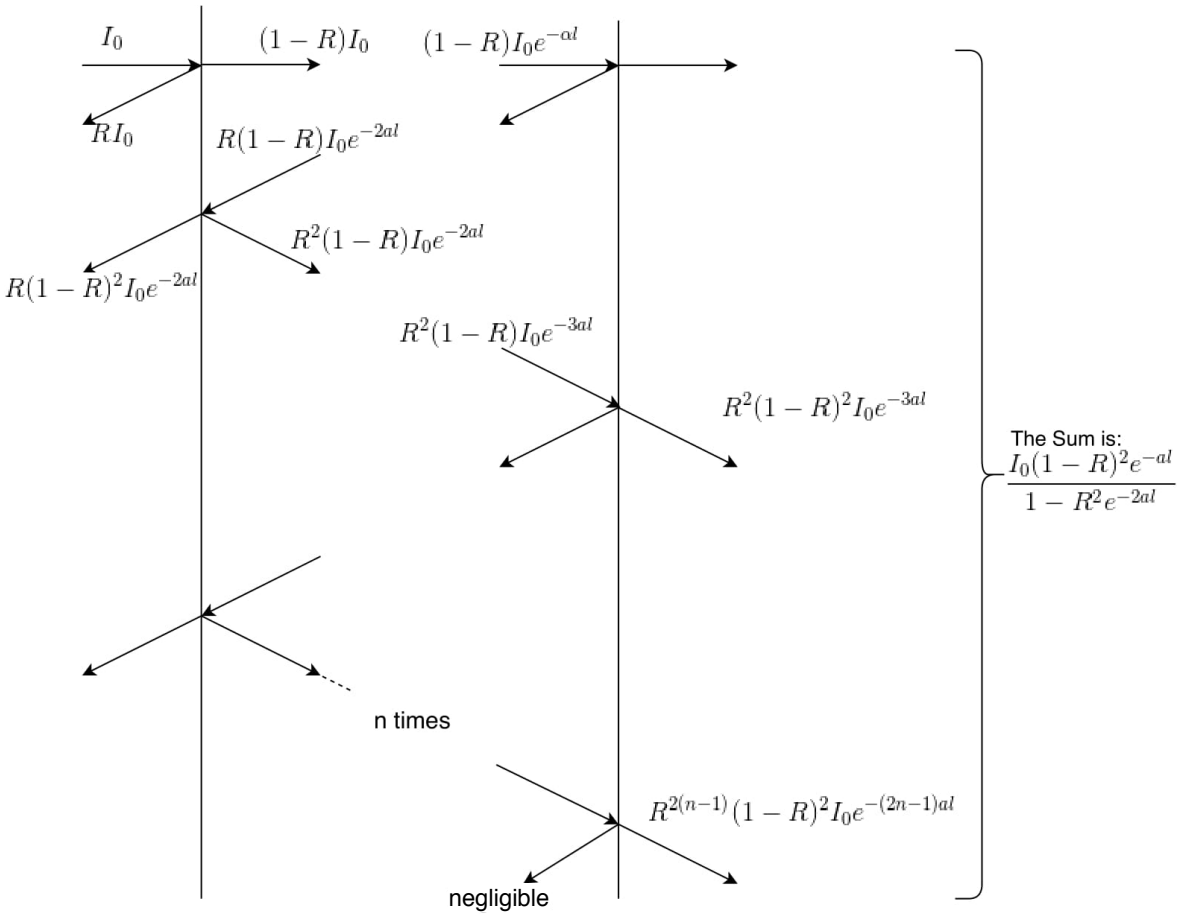

Figure 2.5. Transmission and Internal Reflections.

I_0 is the incident photon intensity, l is the thickness of the semiconductor (GaAs), R is the reflectance of the GaAs, I_T is the intensity of the transmitted light and a is the absorption coefficient with respect to the temperature.

Here we can see that transmission has inverse proportion with the reflection but both of them are wavelength and temperature dependent due to their relationship with the absorption coefficient and refractive index.

Another formula that we need to know is band gap energy changes with the temperature of the GaAs. Formula for the band gap energy with respect to temperature can be seen in following equation by Varshni [67] which is obtained experimentally.

$$\mathbf{E_g}(\mathbf{T}) = E_g(0) - \frac{aT^2}{b+T} \tag{2.5}$$

For example at 300 K , $5.41 \times 10^4 eV/K$ for a and 204 K for b from the literature. a and b are fitting parameters of the Varshni [67] equation and $E_g(0)$ is the band gap energy at room temperature. These values are at $300°K$ temperature.

Equation 2.5 is first found by Varshni [67] At zero kelvin band gap energy is $E_g(0)$, a in (eV/K) and b in (K) are the values that can be determined experimentally. Band gap and temperature relation ship can be seen from the figure 2.6, $E_g(T)$ decreases as the temperature increases. Equation 2.3 which is the absorption coefficient formula shows that band gap energy $E_g(T)$ has also inverse proportion with the absorption coefficient. Finally equation 2.4 for intensity of transmitted light has again inverse proportion with the absorption coefficient.

Equations 2.3, 2.4 and 2.5 gives brief backgroun about understanding the dependence of temperature with the electronic and photonic properties of semiconductor (GaAs) material. We can see that absorption increases with the increasing temperature, thus, transmittance decreases with respect to increasing absorption. As a result,

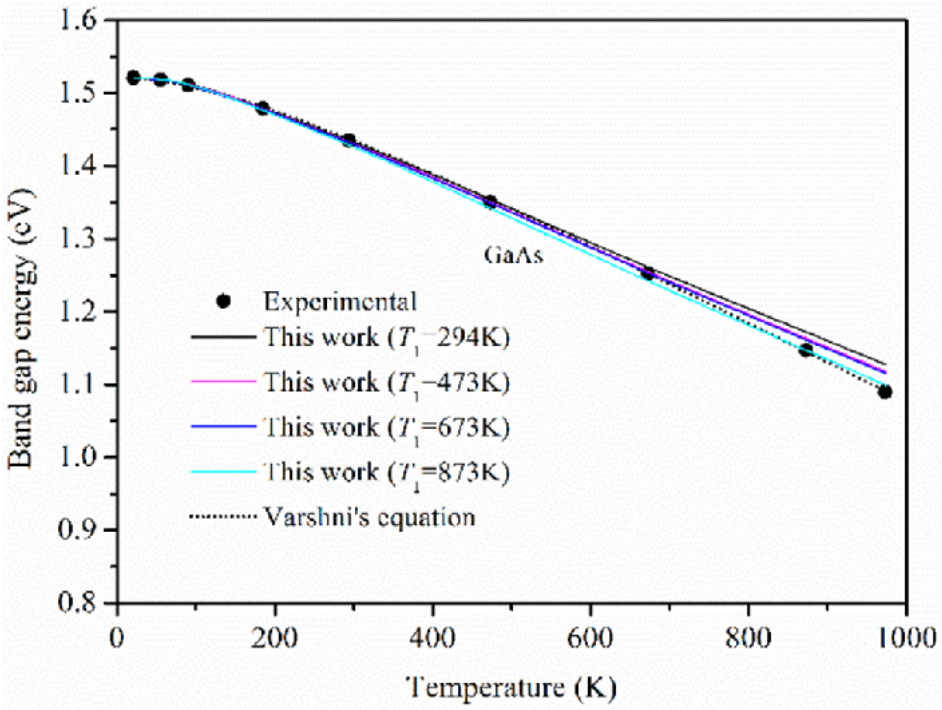

Figure 2.6. Band gap Energy vs Temperature [71]

transmittance decreases as the temperature increases.

Previous formulas were given for understanding the relationship between transmission and temperature.

All stated parameters that gives information about the nature of semiconductor with the light interaction.

Additional information about the reflectance is as follows. The fraction of the light that is reflected depends on the refractive index of the semiconductor (relative to that of air). Reflectance is the reflection of the incident energy from the medium. Incident energy is light according to wavelength. Index of refraction n of the GaAs [72] and index of the air n_{air} are two parameters for calculating reflectance of the semiconductor material which has incident light comes normal to the reflected surface. Figure 2.7 illustrates the behaviour of the light when it come across the interface between air and GaAs. Reflected and transmitted lights has radiant powers which

depends on the refractive indexes of air and GaAs and angle of incidence. Fresnel equations [73] show the relationship between these features and reflected light. To

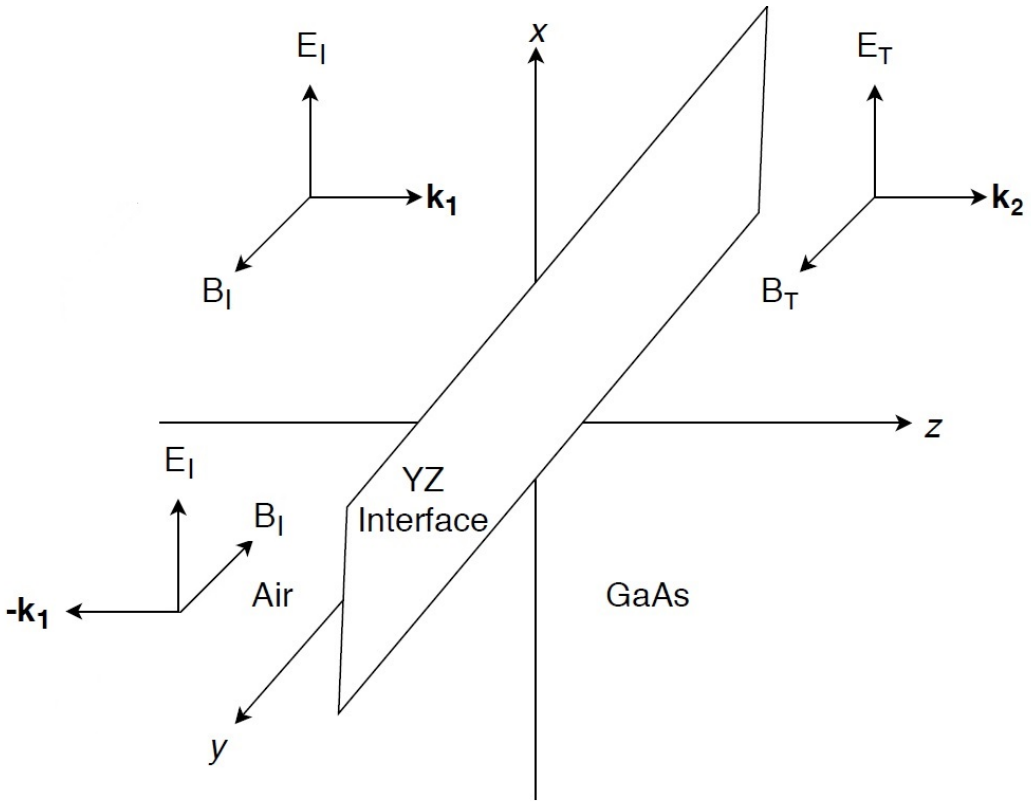

Figure 2.7. Incident, Reflected and Transmitted Lights.

find the Reflectance, we will made some assumptions and derive some equations. We can see the direction propagation vector $\vec{k}$ is z axis in figure2.7. We assume that incident electric field polarized in the x axis direction. According to right hand rule [74], magnetic field is in the y direction. Adding to that, light moves with a speed v_1 in the air and v_2 in the GaAs medium.

We assume Electric and Magnetic field does not change its direction when it transmitted. But their amplitudes change. Again we assume the reflected components of the electric field do not change direction upon reflection, but it travels in the negative z direction. If we apply right hand rule again, we will see that magnetic field goes in the negative y direction.

Electric field of the incoming wave can be described as follows [75]:

$$\vec{E_I} = E_{0i} e^{i(\vec{k}_1 \vec{z} - wt)} \hat{i} \tag{2.6}$$

Where $\vec{E_I}$ is the incident electric field, $\vec{z}$ is the position vector E_{0i} is the amplitude of incident electric field, w is the angular velocity, $i = \sqrt{-1}$, $\hat{i}$ is the unit vector which shows the polarization direction of the electric field in air and $\vec{k}$ is the propagation vector in the air. General formula for the propagation vector is as follows

$$\vec{k} = \hat{k} \frac{2\pi n}{\lambda} \tag{2.7}$$

where n is the index of the refraction, λ is the wavelength in related medium and $\hat{k}$ is the unit vector which shows the direction of $\vec{k}$.

Magnetic field of the incoming wave can be described as follows [75].

$$\vec{B_I} = B_{0i} e^{i(\vec{k}_1 \vec{z} - wt)} \hat{j} \tag{2.8}$$

$\hat{j}$ is the unit vector which shows the polarization direction of the magnetic field and B_{0i} is the amplitude of incident magnetic field.

Reflected components of the wave can be seen in 2.9 and

$$\vec{E_R} = E_{0r} e^{i(-\vec{k}_1 \vec{z} - wt)} \hat{i} \tag{2.9}$$

$\vec{E_R}$ is the reflected electric field and E_{0r} is the amplitude of reflected electric field. Polarization of the electric field does not change but $\vec{k}$ vector is changed in direction which is the reason of the minus sign in front of the $\vec{k}$.

$$\vec{B_R} = -B_{0r} e^{i(-\vec{k}_1 \vec{z} - wt)} \hat{j} \tag{2.10}$$

$\vec{B_R}$ is the magnetic field vector, B_{0r} is the amplitude of the reflected magnetic field. In equation 2.10, we can see that magnetic field changed in both the direction of both $\vec{k}$ and polarization direction which is the reason for the additional minus sign before B_{0r}.

The relationship between electric and magnetic field is can be seen in figure 2.11.

$$\vec{B} = \frac{\vec{E}c}{n} = \frac{\vec{E}}{v} \tag{2.11}$$

c is the speed of light in vacuum, n is the refractive index and v is the speed of light in medium.

We can replace the B_{0r} with $\frac{E_0 r}{v_1}$ according to equation 2.11 where v_1 is the velocity of the light in air. New equation for reflected magnetic field becomes:

$$\vec{B_R} = -\frac{E_{0r}}{v_1} e^{i(-\hat{k}_1 \vec{z} - wt)} \hat{j} \tag{2.12}$$

Tranmitted parts of the wave are shown in equations 2.13 and 2.15.

$$\vec{E_T} = E_{0t} e^{i(\vec{k}_2 \vec{z} - wt)} \hat{i} \tag{2.13}$$

$$\vec{B_T} = B_{0t} e^{(\vec{k}_2 \vec{z} - wt)} \hat{j} \tag{2.14}$$

$\vec{k_2}$ is the propagation vector in GaAs. Speed and wavelength changes in the different medium, this causes incident propagation vector to change from $\vec{k_1}$ to $\vec{k_2}$. According to equation 2.11, transmitted magnetic field becomes:

$$\vec{B_T} = \frac{E_{0t}}{v_2} e^{(\vec{k}_2 \vec{z} - wt)} \hat{j} \tag{2.15}$$

Electric and magnetic components of the incident, reflected and transmitted wave are going parallel to the boundary in the case of normal incidence [76]. In other words, there is no perpendicular component. We will look at the parallel components of the EM wave. Boundary conditions at $z = 0$:

$$\vec{E_I} + \vec{E_R} = \vec{E_T} \tag{2.16}$$

$$\vec{B_I} + \vec{B_R} = \vec{B_T} \tag{2.17}$$

We can simplify the equations 2.16 and 2.17. Taking into account equation 2.11, we can also reformulate the equation 2.17. Simplified equations as follows:

$$E_{oi} + E_{or} = E_{0t} \tag{2.18}$$

$$\frac{E_{oi}}{v_1} - \frac{E_{or}}{v_1} = \frac{E_{0t}}{v_2} \tag{2.19}$$

Due to $\frac{v_1}{v_2} = \frac{n_2}{n_1}$, equations 2.18 and 2.19 can be solved for reflection coefficient r:

$$r = \frac{E_{0r}}{E_{0i}} = \frac{n_1 - n_2}{n_1 + n_2} \tag{2.20}$$

Radiant power P of the wave is proportional to the square of electric field [77] and it can be seen in the formula below

$$P = \frac{E_0^2 \epsilon_0 A}{2v} \tag{2.21}$$

where E_0 is the amplitude of the electric field, A is the area of the electric field, ϵ_0 is the permittivity of vacuum.

Equation 2.21 shows us the relation ship between reflectance R and reflection coefficient r. Reflectance R is the square of r. Reflection formula can be seen as follows:

$$R = [\frac{n_1 - n_2}{n_1 + n_2}]^2 \tag{2.22}$$

If the angle of incidence is greater than zero , assuming that electric field polarized in the x axis and taking the equation 2.11 into account which shows the for relationship between electric and magnetic field, boundary conditions becomes:

$$E_{oi} + E_{or} = E_{0t} \tag{2.23}$$

$$\frac{E_{oi}\cos(\theta_i)}{v_1} - \frac{E_{or}\cos(\theta_r)}{v_1} = \frac{E_{0t}\cos(\theta_t)}{v_2} \tag{2.24}$$

From Snell's law [78], we know that ;

$$n_1 \sin(\theta_i) = n_2 \sin(\theta_t) \tag{2.25}$$

$$n_2 \cos(\theta_t) = n_2\sqrt{1 - \sin^2(\theta_t)} = n_2\sqrt{1 - \frac{\sin^2(\theta_i)}{n_2^2}} = \sqrt{n_2^2 - \sin^2(\theta_i)} \tag{2.26}$$

Substituting equations 2.23 and 2.24 with 2.26 gives us the reflectence for the case angle of incidence (r_{case2}) is greater than zero:

$$r_{case2} = \frac{n_1 \cos(\theta_i) - \sqrt{n_2^2 - \sin^2(\theta_i)}}{n_1 \cos(\theta_i) + \sqrt{n_2^2 - \sin^2(\theta_i)}} \tag{2.27}$$

Reflectance for this case (R_{case2}) is the square of the reflection coefficient:

$$R_{case2} = [\frac{n_1 \cos(\theta_i) - \sqrt{n_2^2 - \sin^2(\theta_i)}}{n_1 \cos(\theta_i) + \sqrt{n_2^2 - \sin^2(\theta_i)}}]^2 \tag{2.28}$$

If we go further in reflectance, it can be seen that reflectance R depends on the refractive index and it is known from literature that refractive index depends on the incoming wavelength [79]. This makes the reflectance a wavelength dependent function.

Refractive index and reflectance data is well reported in the literature. For 980 nm wavelength, GaAs refractive index is 3,5160 at room temperature [80] and refractive index for air is 1 [81]. Refractive index is also temperature dependent but it changes so small in the near infrared which is $2.67 \pm 0.007 \times 10^{-}4/^{\circ}C$ [82]. In detail, refractive index and temperature dependency can be seen in the formula below [82]

$$n(T) = n + \frac{\partial n}{\partial T} T \tag{2.29}$$

where $\frac{\partial n}{\partial T}$ is refractive index variance per degree. Taking n_{gaas}=3,5160 and n_{air}=1, we can calculate the reflectance and use it in further calculations.

$$R = (\frac{3,5160 - 1}{3,5160 + 1})^2 = 0.3103 \tag{2.30}$$

We found R=0.3103 which is almost % 31 of the incident light with normal incidence reflects back at room temperature.

If temperature rises ten degrees from the room temperature, new refractive index becomes for normal incidence;

$$n_{37^\circ C} = 3.5160 + 10 \times 2.6710^{-4} \approx 3.5186 \tag{2.31}$$

At 37°C, reflectance becomes;

$$R = (\frac{3,5186 - 1}{3,5186 + 1})^2 \approx 0.3106 \tag{2.32}$$

Equation 2.32 tells us, $10^\circ C$ temperature rise causes reflected light intensity to increase 0.3%.

2.3. Setup of the Experiment

There are three different setups were done for this experiment.

Setup one has a fiber optic coupled laser source, a 50:50 beam splitter, GaAs

waver at the tip of the beam splitter's fiber cable and photo diode detector for the readings. GaAs were placed to beam splitter's single output side.

There are two different wavelengths were used. First of them is 880 nm, 2.7 (mW) (Min) Fiber-Coupled laser source. This laser source were used in the beginning of the experiments of this thesis. 880 nm near infrared (NIR) is almost at the edge of the cut-off wavelength, which is nearly desired for the setup. Due to the fact that reflection from the semiconductor material is used to detect temperature for the first experiment, 880 nm is used in the setup one. In other words, 880 nm wavelength is enough for transmission theoretically but experimental results can be different from theoretical results. In case of transmission does not occur, reflection thought to be enough to get data with taking into account the absorption.

We use a fiber coupled laser which has 880nm wavelength.In order to drive the 880 nm pigtailed laser source, an appropriate driver is consturcted by using 5 V voltage regulator and passive commponents. Driver schematic and PCB design were done in the the Eagle software. Schematic includes LED driver and transimpedance which converts monitor current from the LED to the voltage. Schematic can be seen in the figure 2.8.

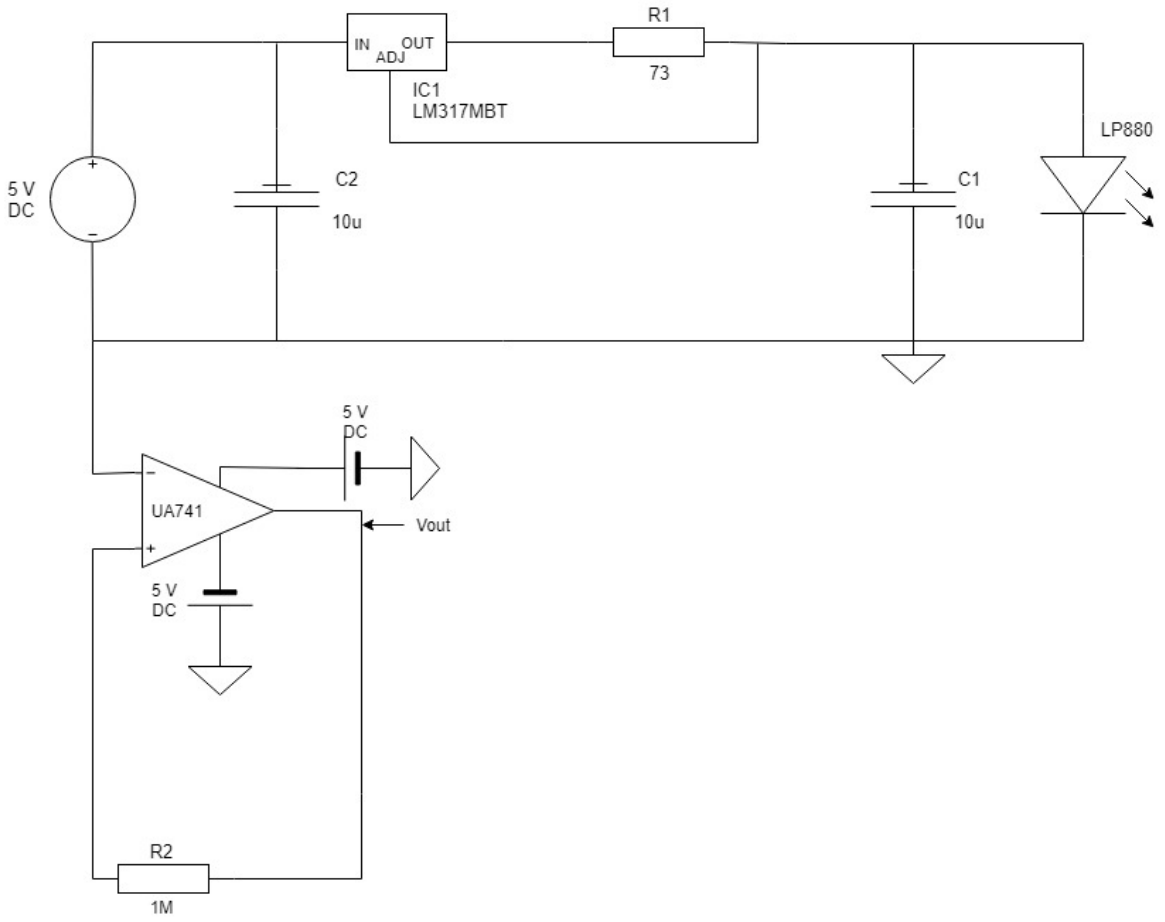

Figure 2.8. Schematic of Laser Driver.

Transimpedance circuit takes the current from the intrinsic photodiode (PD) of the LED. This current goes through the reference resistor which is R2 in the figure 2.8 and induces voltage over R2. This voltage and current from PD will be our reference points when measuring the power of the laser by photo detector.

18mA is required to operate the laser according to its user manual. It is a product from the Thorlabs Inc. (LP880-SF3) and its power is 2.7 mW according to user manual. It has FC/PC connector and its pin code is 'A'. To obtain 18 mA drive current, resistor R1 in figure 2.8 is connected between the output and adjust of the linear voltage regulator. Voltage regulator has constant 1.25 V across the these two nodes. Resistance value can be calculated as follows: $R = \frac{1.25\,(V)}{0.018\,(mA)} \cong 69\Omega$.

We used 73 Ω resistance to get the necessary current to drive the laser diode. Simulation is made for the current through the laser diode. As can bee seen from the figure of simulation 2.9 current is approximately 17.8 mA which is enough to drive the laser diode.

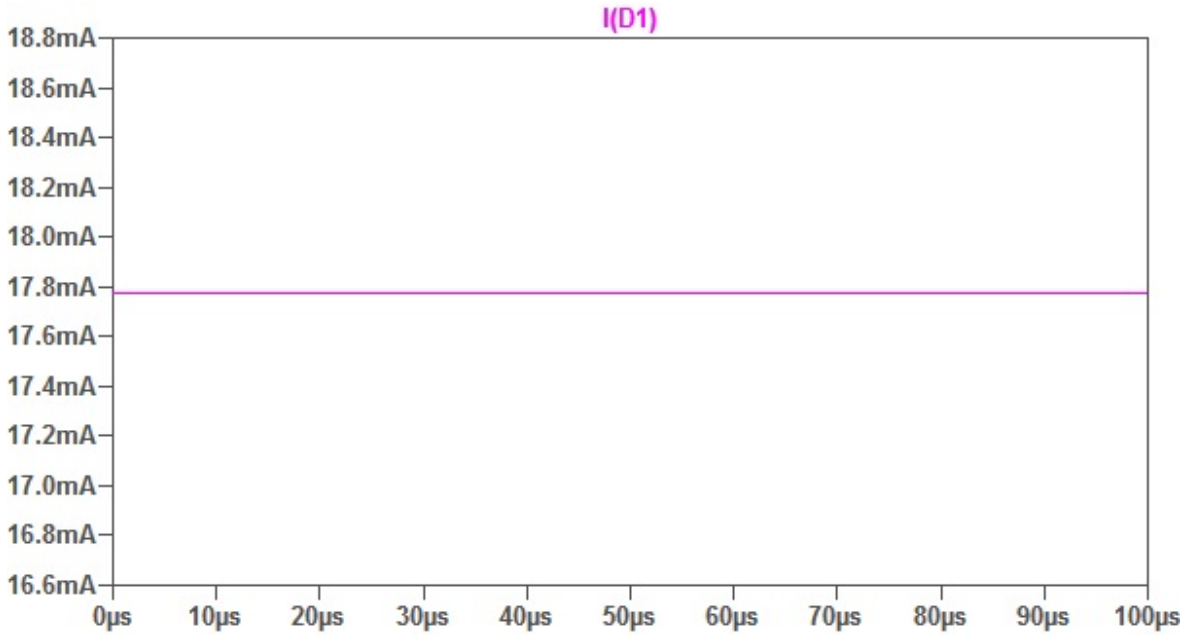

Figure 2.9. Simulation Result of the Current Passing over the Laser Diode.

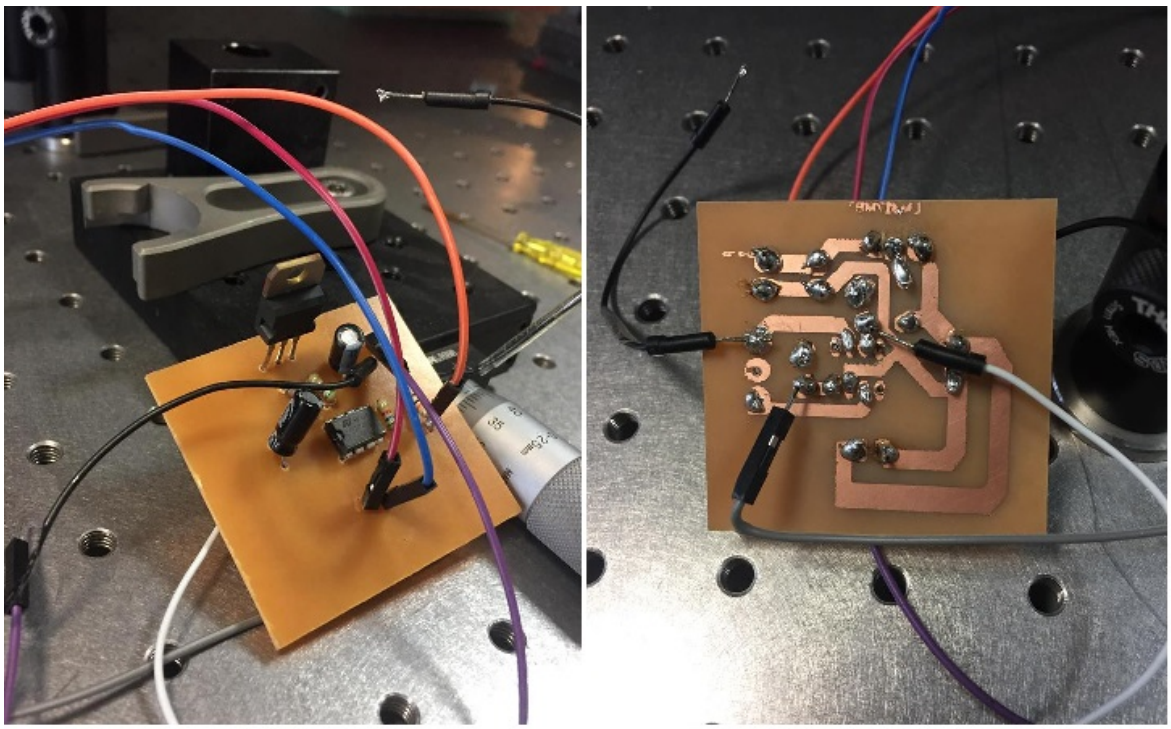

Figure 2.10. Rear and Front View of the Laser Driver.

Figure 2.10 is the photo of the laser driver.

The intrinsic photo diode on the laser gives the 0.22 mA monitor current when the device is fed with the operating current according to user manual. PD current is converted to the voltage via simple transimpedance circuit. Converting the monitor current to the voltage provide us a reference point when comparing the power measured from the power meter.

Optical kit used for the whole experiment is PM120VA which has the analog/digital optical meter PM100A. It is a product from Thorlabs Inc and its measurement range can easily handle with the power ranges in the experiments of the thesis.

Heating and cooling was a little bit hard due to the fact that when we heat or cool down to a semiconductor, it is really hard to maintain the temperature in same levels. Deciding the method for cooling the semiconductor to $-6°C$ is not that easy due to gallium arsenide fragile nature. Stabilization of the temperature at the same level needs a professional tool such as heating and cooling chamber which would be better for the experiments.

Methods for heating and cooling processes that are used in the experiments are explained as follows.

Heating was handled by using a peltier for setup one and two, hot air compressor for setup three. Cooling process was hard to achieve. First, peltier thermoelectric cooler (TEC 12706) was used to cool down the gallium arsenide but infrared laser never gave us the value below 15°C. To reach lower temperatures, another method for cooling was found and prepared. Peltier thermoelectric cooler and 12 V mini fan were used inside an insulated polystyrene box. Polystryrene box is a very good heat insulator. This time, temperature stabilization achived but temperature never went down below 10°C.

Finally cooling process were reached to the desired temperatures with the help of freezer spray. Freezer spray was chosen to be the better option to go down further degrees. For setup one and two, peltier temperature reduced below zero degrees with the help of the freezer. Freezer was never interact with the GaAs wafer or photodiode. For the setup three, freezer spray were used directly to the GaAs wafer. Firstly, freezer is tested without GaAs semiconductor to see if it is affecting the photo diode or not. It was observed that spraying through the photo diode and laser source did not change the value at the analog/digital power meter display. Then the setup was prepared in a way to protect the photodiode from the freezer spray. Protection were done to keep clean the surface of the photodiode.

Stabilization of the temperature was a desired condition but another option was used during the experiments. Videos of the experiments were recorded instead of

stabilizing the temperature. It was an effective way to keep track temperature and power values and of course faster than the stabilizing the temperature at some point. Video can be stopped and data can be observed at any time without missing any part of it.

For the setup setup three, we measured the transmission. We used different wavelength for setup two and three. Because there was no transmission observed through the GaAs wafer in setup one. 980 nm laser source was chosen instead of 880 nm laser diode. 980 nm laser still does not meet with our expectations due to the chosen semiconductor wafer specifications but it was helpful in observing the changes in transmission.

Second setup consist of 980 nm wavelength laser source as mentioned with approximately 23.8 mW lsaer power. 980 nm LED is chosen for the rest of the experiment.

Besides of 980 nm laser source, a peltier cooler and freezer were used for the cooling and heating process. Second experiment depends on the reflection from the surface of the GaAs semiconductor through the air and detection of the reflected light by the photodetector.

Schematics of the setup one and two can be seen in figure 2.11.

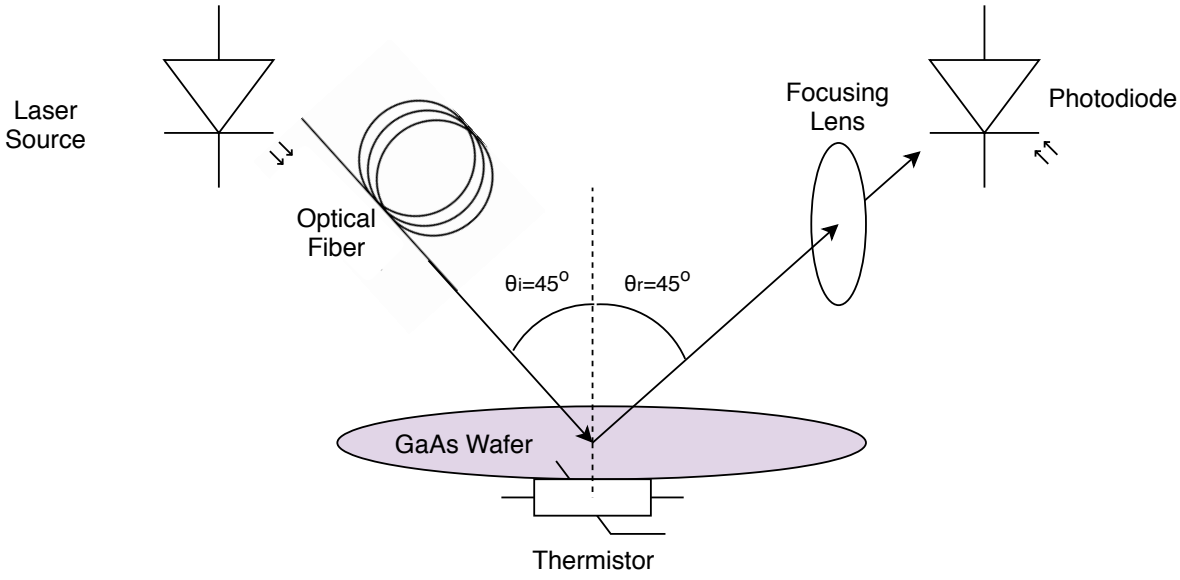

Figure 2.11. Schematic of the Setup One and Setup Two.

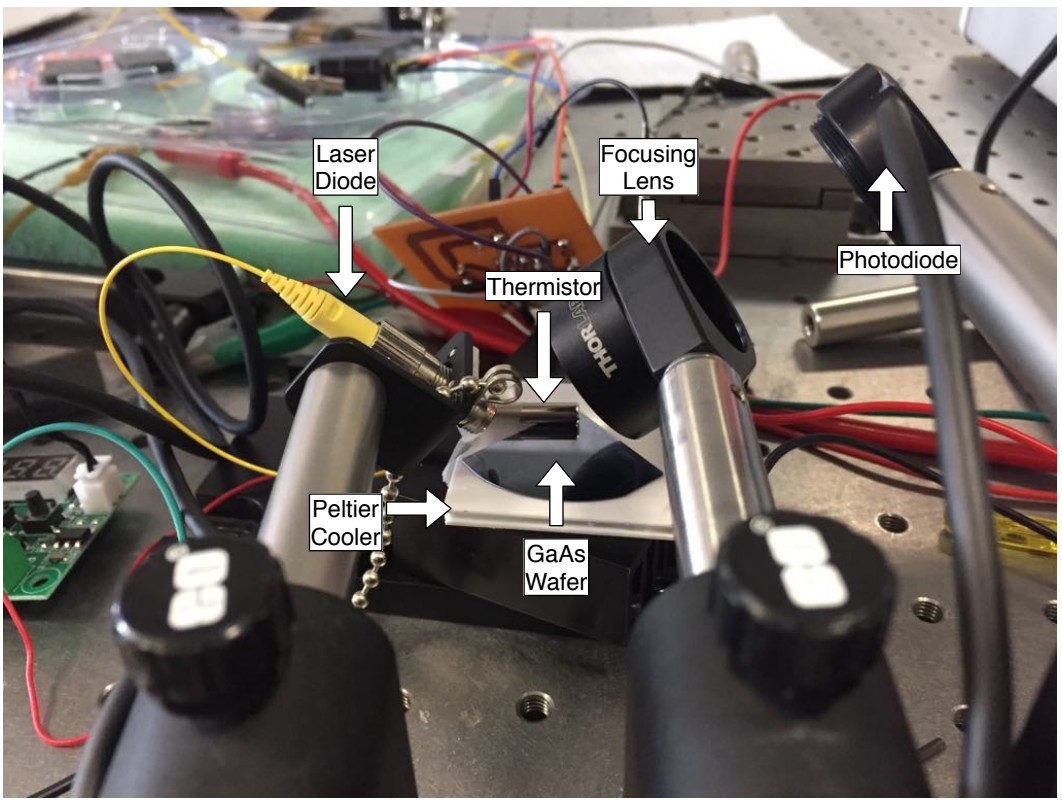

Figure 2.12. Setup One.

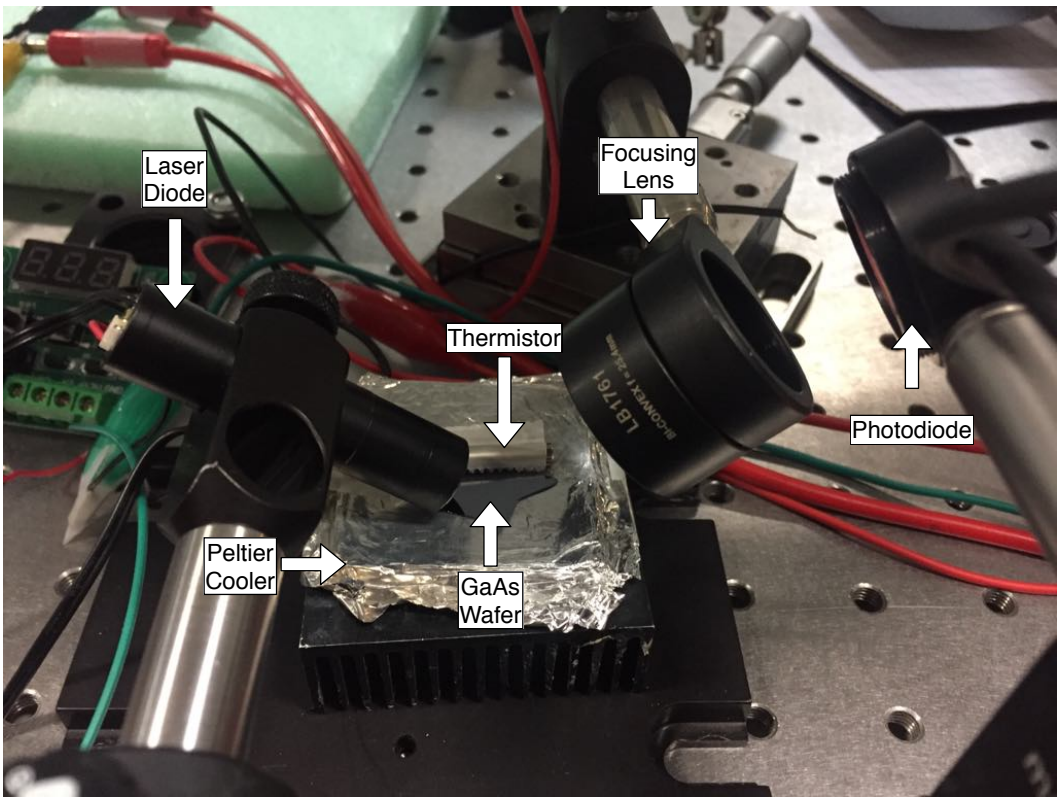

Figure 2.13. Setup Two.

Third and last setup is based on the transmission power of the 980 nm light through the GaAs. This transmission will have a role at the further experiments for other researches besides of this thesis.

Setup three has 980 nm laser pointer source fixed on the table. GaAs wafer is fixed between the 980 nm wavelength laser pointer and the photodiode. 5 V DC is applied to drive the laser pointer.

We can see the schematic and photo of the setup three in figures 2.14 and 2.15 respectively.

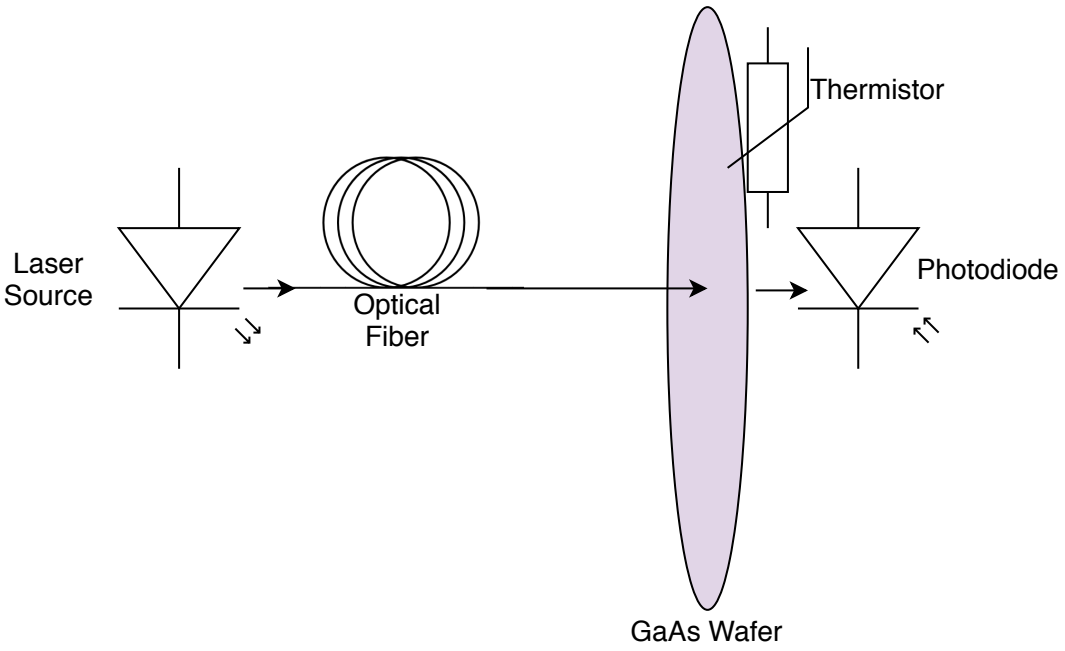

Figure 2.14. Schematic of the Setup Three.

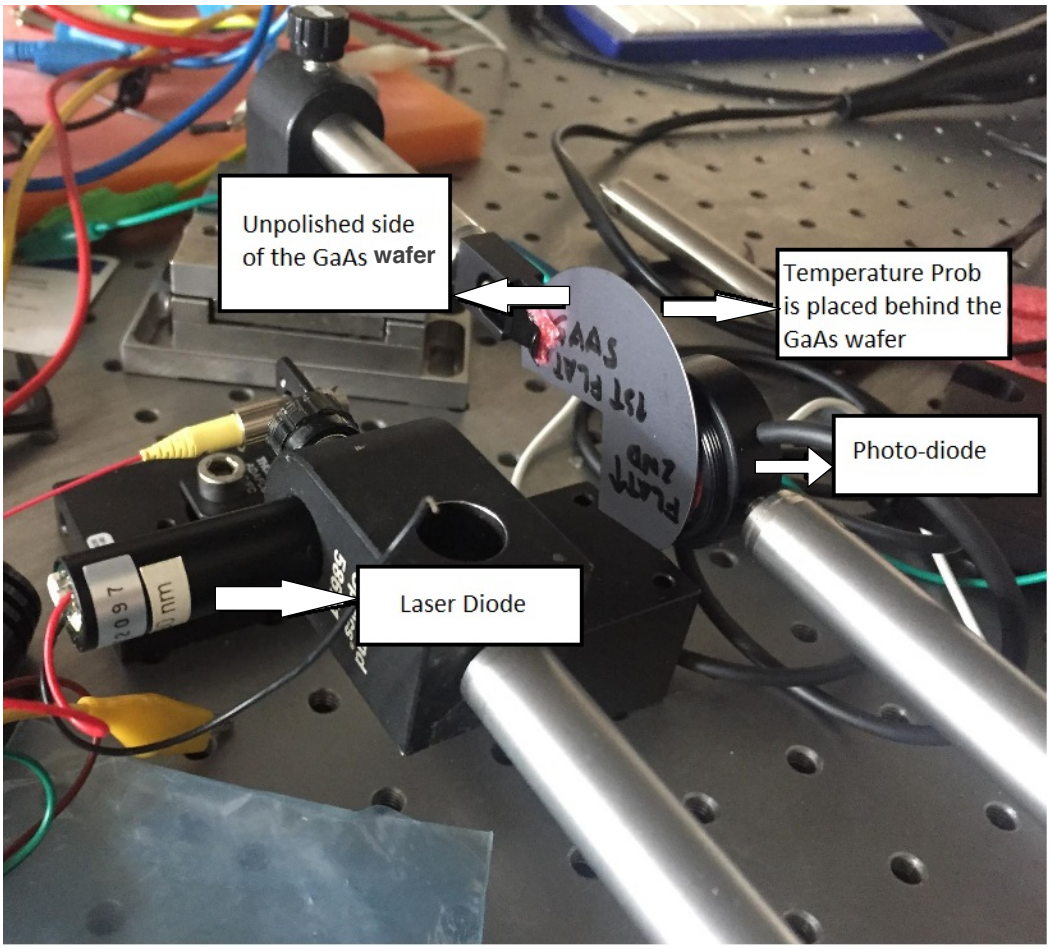

Figure 2.15. Setup Three.

3. RESULTS

Heating and cooling processes were done without harming the exit point of the fiber cable and equipments.

Setup three does not consist of any focusing lenses due to illuminated light goes directly to the GaAs and GaAs is adjacent to photodiode. Focusing lens also were used in the setup three but no difference were observed from the setup with no focusing lens.

3.1. Setup One Results

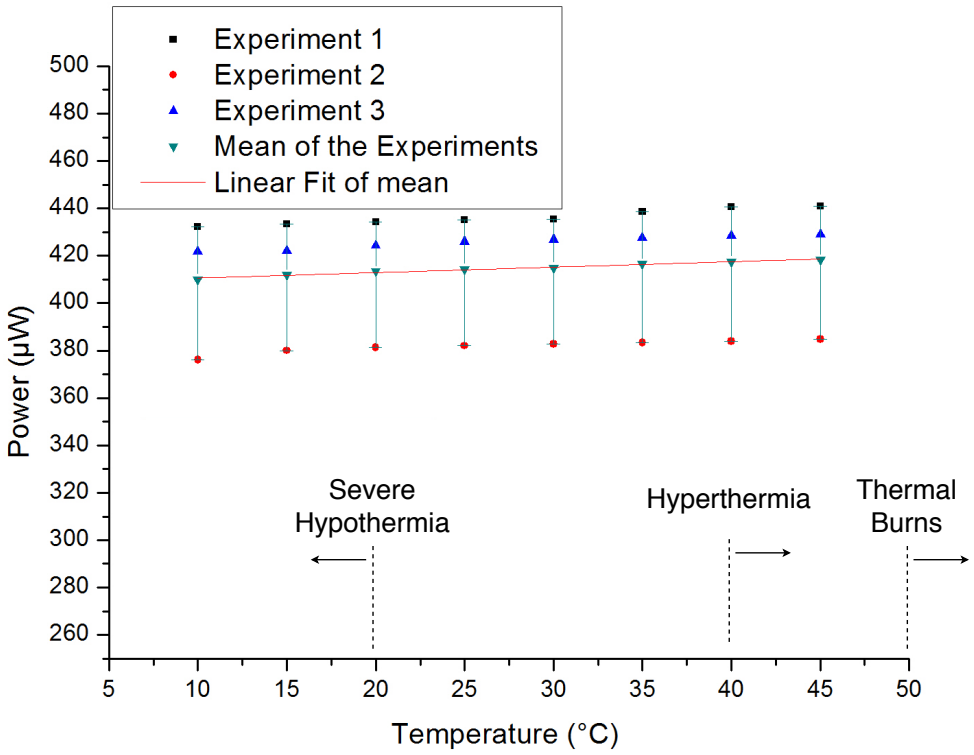

Figure 3.1. Reflected Power vs Temperature.

In setup one, reflectance change over the temperature can be calculated from the formula 2.18:

For $27°C$, and $45°$ incident angle:

$$R_{case2} = [\frac{3,516cos(45) - \sqrt{1^2 - sin^2(45)}}{3,516cos(45) + \sqrt{1^2 - sin^2 45}}]^2 = 0,3103 \tag{3.1}$$

For $37°C$, incex of refraction becomes;

$$n_{37°C} = 3.5160 + 10 \times 2.67 \times 10^{-4} \approx 3.5186 \tag{3.2}$$

New reflectance for $37°C$ with $45°$ incident angle can be calculated as follows:

$$R_{case2} = [\frac{3,5186\cos(45) - \sqrt{1^2 - \sin^2(45)}}{3,5186\cos(45) + \sqrt{1^2 - \sin^2(45)}}]^2 \approx 0,3106 \tag{3.3}$$

Just like the normal incidence case, reflectance changes 0.3%.

We saw that 880 nm laser source has $1.210(mW)$. Average power of the reflected light for the room temperature is $414.36\mu W$ which is almost 34% of the incident light. A change of 0.3% in incident light corresponds to a change of $3.63\mu W$ in reflected light. This means $0.363\mu W$ change per degree. This value is so small to detect, so we measured it in every $5°C$. In figure 3.1, this small change can be observed. On avarage, $2.36\mu W$ is observed for every $10°C$.

3.2. Setup Two Results

Just like the setup one, 0.3% change should be observed in every ten degrees. Laser source has 23.8 mW and 0.3% change corresponds to $71.4\mu W$ change in reflected light for $10°C$ change. Our average result is approximately $59.7\mu W$. Reflected light is the 32.6 % of the incident light at room temperature.

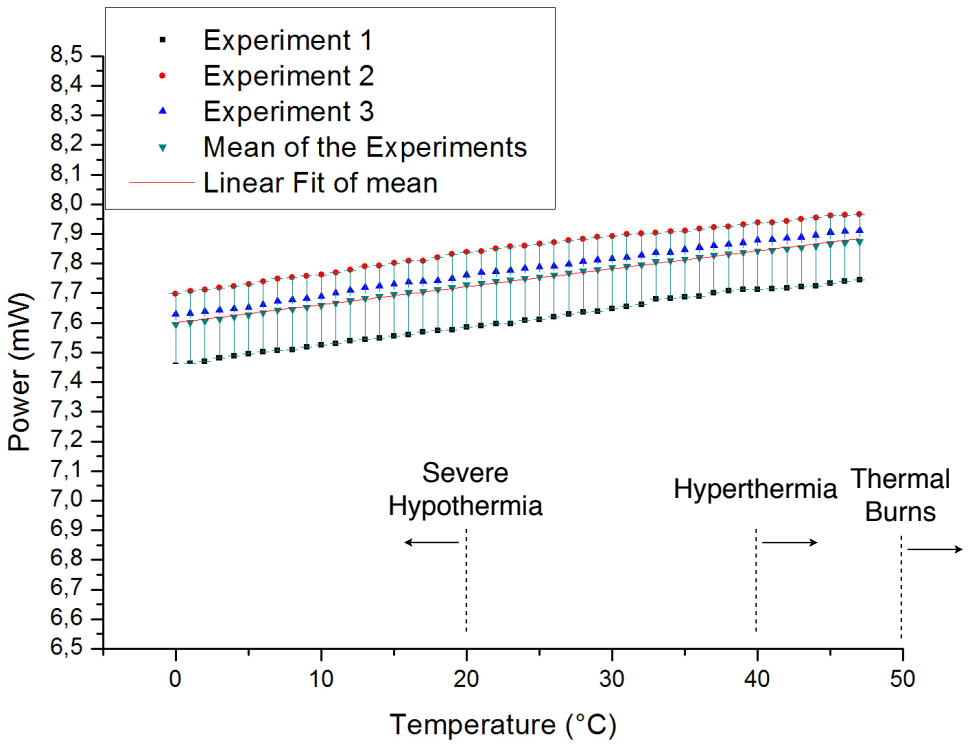

Figure 3.2. Reflected Power vs Temperature.

3.3. Setup Three Results

Data taken from the $-6°C$ to $50°C$.

We can see the results of setup three in the figure 3.3.

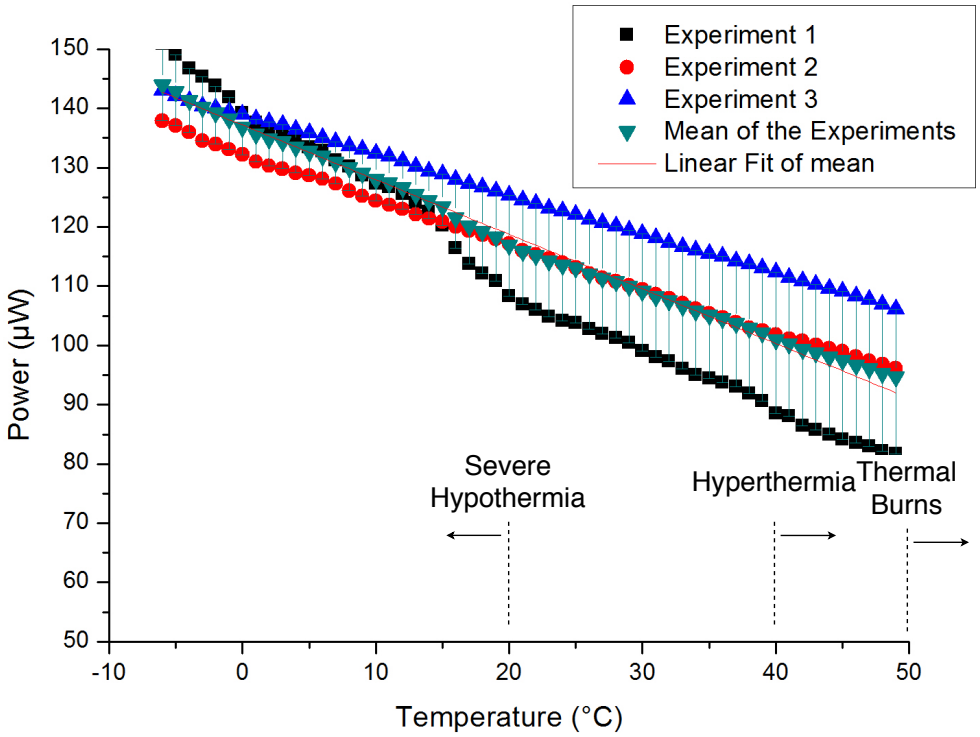

Figure 3.3. Transmitted Power vs Temperature.

When the body is below $20°C$, severe hypothermia occurs which is organs start to fail, heart rate falls to risky levels as in respiration [83]. Normal body temperature is $37°C$ [84]. Hyperthermia [85] damages the enzymes such as respiration enzymes which is responsible for cellular respiration [86] fail to work in the body. Tissue burns start at $50°C$ [87].

It can be clearly seen that transmitted power has a linear relationship with the changing temperature which is desirable for temperature tracking.

3.3.1. Analysis of the Results

In Setup one, output power of the laser source was different from the user manual as well as the intrinsic photodiode of the laser. Transmission through the GaAs was almost zero and we measure the reflected light power. Reflectance change over the temperature is $2.36\mu W$ in every $10°C$ which is a little bit low from the expected variance. Linear relationship between the reflected light power and temperature was observed.

In Setup two, 980 nm laser source was used. Variations in the reflected light was more observable than the setup one. On average variation was $59.7\mu W$ per ten degrees which is close to expected variation. Setup two was easy to read results on the powermeter due to its bigger variations with the temperature which is more detectable by photodiode. Linear relationship between the reflected light power and temperature was observed just as setup one.

In setup three, temperature dependence of the transmitted light power was observed. We were expecting more transmission from our results. Reasons for low transmission were explained below.

3.3.1.1. Reasons of Low Transmission. One can be recognize that transmission is too low which is around between 0.4% and 0.5% of the laser power (23.8 mW) at room temperature. We know from the literature that in the range of 980 nm wavelength, transmission should be much more than our results.

There are some reasons behind our low transmission, first of all GaAs wafer used in the experiment has only one side polished. Wafer polishing is important in optic experiments. Wafer polishing process removes surface defects [88] and make the wafer particle free. Smoothing the surface peaks and valleys are important factor. This peaks and valleys can be a couple of micron in size but they have quite badly affect on the transmission [89]. Due to defects on the unpolished side, incoming light reflects back

and disperse widely and transmission decreases to the levels of between 0.4%-0.5% of laser power (23.8 mW).

As an example to effects of comparing the transmissions between single side polished and double side polished wafers, the following figure 3.4 shows us the transmission rates of the single side polished versus double side polished silicon wafer. Red line shows the single side polished (SSP), blue line shows the double side polished (DSP) and the black line represents the reference transmission without any wafer between laser source and photodiode. Almost 90% of the transmission is lost in the infrared region for the single side polished wafer because of the diffusion and scattering of the transmitted and reflected light.

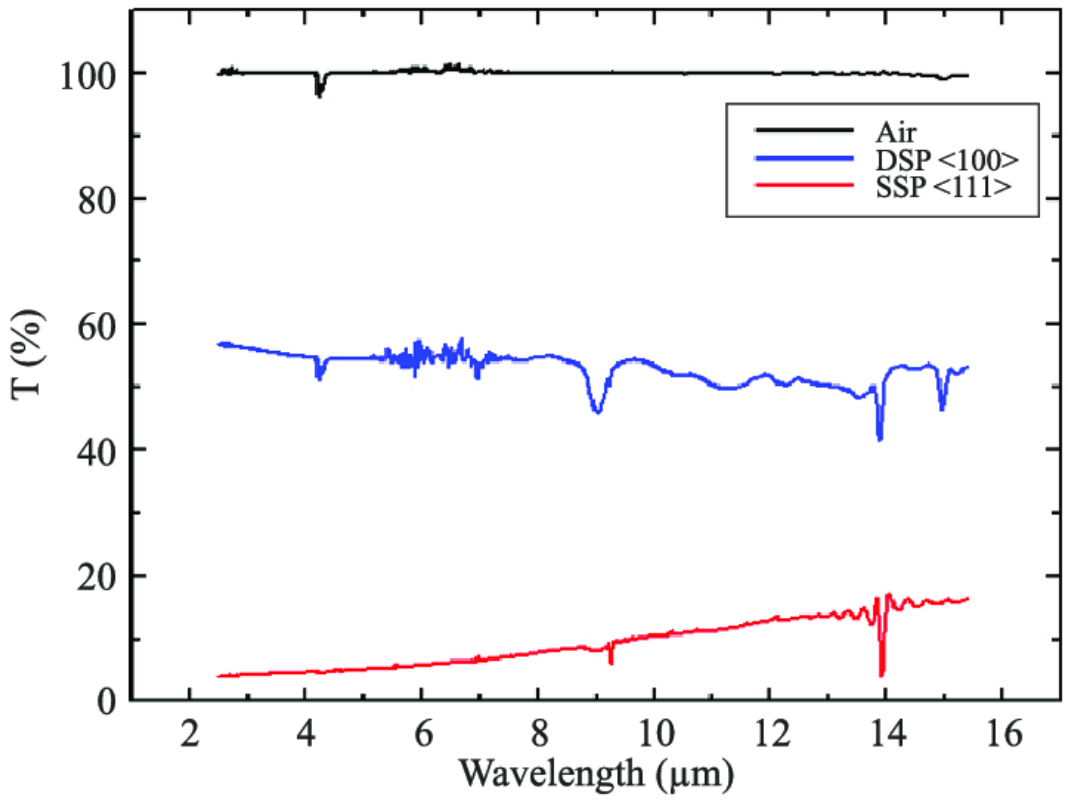

Figure 3.4. Single Side Polished vs Double Side Polished Wafer Transmission [89]

Critical angle is the greatest angle before the total reflection occurs as the light goes from the medium with higher refractive index to the medium with lower refractive index [11]. Most of the reflected light from the unpolished side scatters inside the

critical angle and escapes through the polished side. A large part of the light is trapped inside due to their angle of incidence is larger than the critical angle [11].

This scattering and diffusion from the unpolished side of the wafer were seen in the experiments of the thesis. When we tried to measure the reflected light from the unpolished side of the wafer, photodiode did not get any noticeable results.

In the figure 3.5, we can see the diffused reflected light from the unpolished side of the wafer. Calculating and modeling the scattered light from the rough surface is really hard even if elaborated information about the rough surface is known.

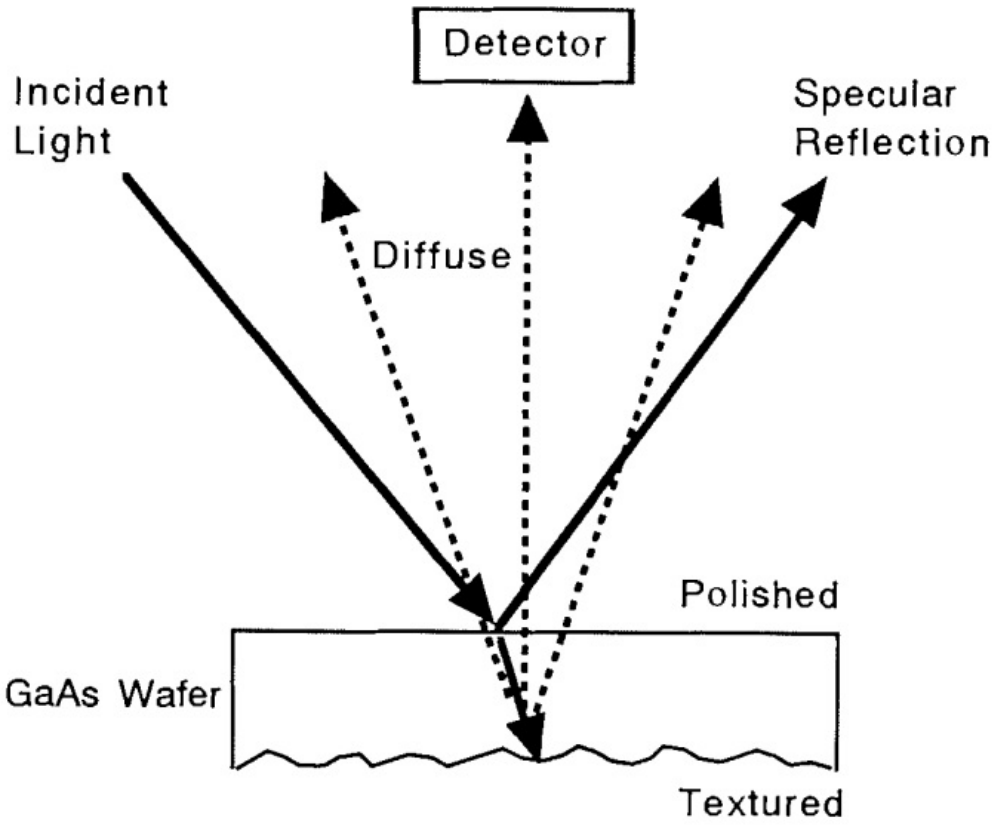

Figure 3.5. Diffuse Reflectivity of the Single Side Polished Wafer [90].

Second reason for such a low transmission is wafer does not have an antireflection coating (AR). Anti reflection coating decreases the reflectance around 4% [91] and contribute to the transmission of illuminated light.

Third reason is thickness. Thickness is important parameter for transmission. Thickness and transmittance relation can be seen simply in Lambert-Baer´s Law [70] in the formula 3.4

$$T = e^{-al} \tag{3.4}$$

Where T transmittance, a is the absorption coefficient with respect to temperature and l is the thickness. Thickness and transmittance relationship were demonstrated in figure 2.4. As the thickness increase, transmitted power decreases. If we had use thinner wafer than ours, our transmitted power would be much more than the results of current one.

These unwanted properties of the GaAs wafer were due to the misleading informations from the wafer supplier company that sold us the GaAs wafer.

4. CONCLUSION

4.1. Conclusion

In this thesis, transmission and absorption of the gallium arsenide has been studied. Background and applications of fiber optic temperature sensors were introduced in Chapter 1. Especially medical applications were emphasized due to aim of this thesis. Usage areas of FOTSs in medical area has been introduced widely. Besides medical industry, other areas also has been metioned shortly due to that FOTSs can be used in many fields. In addition to that, advantages of the fiber optic sensors have been explained and contributions of the thesis have been written item by item. Advantages of the FOTSs provides to FOTSs more market area and followed by faster technological developments which moves FOTSs one step further.

In Chapter 2, Firstly, gallium arsenide pysical and optical properties were introduced to show it suitability to this thesis. The reasons for choosing gallium arsenide as a appropriate semiconductor to make a fiber optic sensor have been explained. Its band gap energy changes with respect to temperature presented in the formulas. Temperature and transmission dependence has been shown thanks to these formulas and their inventors; Urbach's rule [69] and Varshni equation [67]. Relationship between formulas has been shown and dependencies between temperature, bandgap, absorption and transmission have been correlated. After introducing the theoretical formulas, setups for the experiments were explained in detail. Finally, refractive index was taken as 3,516 from the Skauli et al. 2003 [80]. Some GaAs refractive index values can be different from each other but this differences only change some calculations but important factor in the thesis is seeing dependence of band gap and transmission to the temperature.

In Chapter 3, different transmitted power with different temperatures have been shown. Cooling and heating results have been introduced. Cooling and heating have been tried in a different way such as Peltier cooler itself and Peltier cooler and a fan in

a polyester box in the beginning of the experiments but achieving desired temperatures were really hard with the Peltier cooler or its derivatives. Although the mechanism for cooling and heating we choose seems simple, it was really helpful in our experiments and there was no harmful effect on the gallium arsenide wafer and photodiode. We did not go any furhther below from $-10°C$ or upper from $50°C$ to prevent any possible damages on the photodiode. Additionally, transmitted power were low compared to literature. Reasons behind this low transmission have been explained.

4.2. Future Work Advices

Here some advices for future works. Some of these recommendations have been learned by searching, but most of them have been learned by making mistakes and misunderstandings between us and the wafer supplier.

- Choosing the right semiconductor is quite important such experiments. Polishing both sides of the semiconductor wafer is important for transmission experiments. Also thickness is an important parameter like 2 side polishing.
- Right laser source is another important factor for transmission measuring. One has to calculate the cut-off wavelength and choose the laser source wavelength higher or equal to calculated wavelength if only one wavelength is used.
- Gallium arsenide or any other wafers in such experiments should be treated very carefully. Dust particles or other things can leave marks on the wafer. These marks can be cleaned by acetone with sanitary napkins. One should not clean the wafer in his/her hands or otherwise wafer will shatter in a high probability. Wafer should be clean on the soft surface.
- If the GaAs wafer or another type of wafer is cut into two or more parts, it's orientation should be considered. Wafer can be cut by simple diamond cutting saw. From wafer's orientation, cutting direction should be known. Cutting process should be learned before cutting the wafer because diamond cutting wafer should be pressed only one point, and rest of the crack occurs by itself very smoothly along it's orientation.

- Transmission observations can be done in better environments. If the semiconductor wafer can be placed in a professional heating cooling equipment, temperature can be stabilized and observations become clearer. Cooling with freezer spray is an alternative but every time gallium arsenide has to be cleaned after spraying.

REFERENCES

1. Schena, E., D. Tosi, P. Saccomandi, E. Lewis and T. Kim, "Correction: Schena, E.; et al. Fiber Optic Sensors for Temperature Monitoring during Thermal Treatments: an Overview. Sensors 2016, 16, 1144", *Sensors*, Vol. 18, No. 4, p. 1226, 2018.

2. Inaudi, D. and B. Glisic, "Fiber Optic Sensing for Innovative Oil and Gas Production and Transport Systems", *Optical Fiber Sensors*, p. FB3, 2006, `http://www.osapublishing.org/abstract.cfm?URI=OFS-2006-FB3`.

3. Vidonish, J. E., K. Zygourakis, C. A. Masiello, G. Sabadell and P. J. Alvarez, "Thermal Treatment of Hydrocarbon-Impacted Soils: A Review of Technology Innovation for Sustainable Remediation", *Engineering*, Vol. 2, No. 4, pp. 426 – 437, 2016, `http://www.sciencedirect.com/science/article/pii/S2095809917300796`.

4. Becker, J. A., C. B. Green and G. L. Pearson, "Properties and uses of thermistors ; Thermally sensitive resistors", *The Bell System Technical Journal*, Vol. 26, No. 1, pp. 170–212, January 1947.

5. Ogura, H., J. Tamba, M. Izuchi and M. Arai, "Effect of temperature distribution on EMF of thermocouples", *Proceedings of the 41st SICE Annual Conference. SICE 2002.*, Vol. 1, pp. 498–500 vol.1, Aug 2002.

6. Narayanaswarny, R., "Optical sensors", *2005 Asian Conference on Sensors and the International Conference on New Techniques in Pharmaceutical and Biomedical Research*, pp. 1–4, September 2005.

7. Popovic, B. D., "Electromagnetic field theorems", *IEE Proceedings A - Physical Science, Measurement and Instrumentation, Management and Education - Reviews*, Vol. 128, No. 1, pp. 47–63, March 1981.

8. Nara, K., "Study of the Magnetic Field Effect on Commercial Thermistors using a Water Triple Point", *Japanese Journal of Applied Physics*, Vol. 44, No. 3R, p. 1506, 2005, http://stacks.iop.org/1347-4065/44/i=3R/a=1506.

9. Scanlon, P. J., R. N. Henriksen and J. R. Allen, "Approaches to Electromagnetic Induction", *American Journal of Physics*, Vol. 37, No. 7, pp. 698–708, 1969, https://doi.org/10.1119/1.1975777.

10. Sabri, N., S. A. Aljunid, M. S. Salim, R. B. Ahmad and R. Kamaruddin, "Toward Optical Sensors: Review and Applications", *Journal of Physics: Conference Series*, Vol. 423, No. 1, p. 012064, 2013, http://stacks.iop.org/1742-6596/423/i=1/a=012064.

11. Jarvis, P. R. and G. H. Meeten, "Critical-angle measurement of refractive index of absorbing materials: an experimental study", *Journal of Physics E: Scientific Instruments*, Vol. 19, No. 4, p. 296, 1986, http://stacks.iop.org/0022-3735/19/i=4/a=010.

12. Václav Škoda, J. V., "A study of metal-dielectric mirrors technology with regard to the laser-induced damage threshold", *Proc.SPIE*, Vol. 10014, pp. 10014–10014–5, 2016, https://doi.org/10.1117/12.2245191.

13. Russo, R. E., "Laser Ablation", *Appl. Spectrosc.*, Vol. 49, No. 9, pp. 14A–28A, September 1995, http://as.osa.org/abstract.cfm?URI=as-49-9-14A.

14. Mallard, J. R., "Magnetic Resonance Imaging (MRI) x2014; The odyssey of one contributor to its birth", *1992 14th Annual International Conference of the IEEE Engineering in Medicine and Biology Society*, Vol. 7, pp. 2860–2862, October 1992.

15. Dichen, L. and C. Yan, "Study of interference and damage experiments on electronic equipment in transient and stable EM field", *2002 3rd International Symposium on Electromagnetic Compatibility*, pp. 308–313, May 2002.

16. Rice, T., S. Poland, B. Childers, M. Palmer, J. Elster, B. Fielder, D. Maleski and M. Gunther, "Fiber Optic Temperature Sensors—A New Temperature Measurement Toolbox", *AIP Conference Proceedings*, Vol. 684, No. 1, pp. 1015–1020, 2003, http://aip.scitation.org/doi/abs/10.1063/1.1627262.

17. Eden, R. C. and P. D. Coleman, "Proposal for microwave modulation of light employing the shift of optical absorption edge with applied electric field", *Proceedings of the IEEE*, Vol. 51, No. 12, pp. 1776–1777, December 1963.

18. Yoshitomi, K., "Schrödinger operators with periodic potentials and constant magnetic fields with integer flux", *Osaka J. Math.*, Vol. 34, No. 4, pp. 859–893, 1997, https://projecteuclid.org:443/euclid.ojm/1200787786.

19. Gräfe, W., *The Model of Kronig and Penney*, pp. 9–13, Springer International Publishing, Cham, 2015, https://doi.org/10.1007/978-3-319-19764-7$_2$.

20. Hobden, M. V. and M. D. Sturge, "The Optical Absorption Edge of Gallium Arsenide", *Proceedings of the Physical Society*, Vol. 78, No. 4, p. 615, 1961, http://stacks.iop.org/0370-1328/78/i=4/a=119.

21. Szweda, R., "6 - Gallium Arsenide Crystal Growth", R. Szweda (Editor), *Gallium Arsenide (Third Edition)*, pp. 147 – 160, Elsevier Science, Oxford, third edition edn., 2000, http://www.sciencedirect.com/science/article/pii/B9781856173643500078.

22. Kao, K. C. and G. A. Hockham, "Dielectric-fibre surface waveguides for optical frequencies", *Electrical Engineers, Proceedings of the Institution of*, Vol. 113, No. 7, pp. 1151–1158, July 1966.

23. Maiman, T. H., "Stimulated Optical Radiation in Ruby", *Nature*, Vol. 187, pp. 493 EP –, Aug 1960, http://dx.doi.org/10.1038/187493a0.

24. Udd, E., "An overview of fiber optic sensors", *Review of Scientific Instruments*,

Vol. 66, No. 8, pp. 4015–4030, 1995, https://doi.org/10.1063/1.1145411.

25. Kersey, A. D., "A Review of Recent Developments in Fiber Optic Sensor Technology", *Optical Fiber Technology*, Vol. 2, No. 3, pp. 291 – 317, 1996, http://www.sciencedirect.com/science/article/pii/S106852009690036X.

26. Ruffin, P. B., "A review of fiber optics technology for military applications", *Proc.SPIE*, Vol. 10299, pp. 10299 – 10299 – 24, 2000, https://doi.org/10.1117/12.419796.

27. Qiao, X., Z. Shao, W. Bao and Q. Rong, "Fiber Bragg Grating Sensors for the Oil Industry", *Sensors*, Vol. 17, No. 3, p. 429, 2017.

28. Voet, M. R. H., Y. Verbandt and F. Berghmans, *Fibre Optic Sensors: Potential, applications and state of the art of the technology*, pp. 647–689, Springer Netherlands, Dordrecht, 1995, https://doi.org/10.1007/978-94-011-0035-9$_3$3.

29. Taffoni, F., D. Formica, P. Saccomandi, G. Pino and E. Schena, "Optical Fiber-Based MR-Compatible Sensors for Medical Applications: An Overview", *Sensors*, Vol. 13, No. 10, p. 14105–14120, 2013.

30. Shi, W., K. Shen, J. K. Li, G. H. Sigel and R. Mezrich, "Fiber optic sensors for biomedical measurements in magnetic resonance imaging (MRI)", *Proceedings., 39th Electronic Components Conference*, pp. 479–481, May 1989.

31. Zhu, Y. and A. Wang, "Miniature fiber-optic pressure sensor", *IEEE Photonics Technology Letters*, Vol. 17, No. 2, pp. 447–449, February 2005.

32. Betta, G. and A. Pietrosanto, "An intrinsic fiber optic temperature sensor", *IEEE Transactions on Instrumentation and Measurement*, Vol. 49, No. 1, pp. 25–29, February 2000.

33. Nagaike, Y., G. Lai, Y. Wu and H. Ikeda, "Sub-micron position sensor with a fiber-

optic interferometer", *Conference Record of the 1999 IEEE Industry Applications Conference. Thirty-Forth IAS Annual Meeting (Cat. No.99CH36370)*, Vol. 3, pp. 1751–1753 vol.3, 1999.

34. Harald Bueker, F. W. H., "Fiber optic radiation sensors", *Proc.SPIE*, Vol. 2425, pp. 2425 – 2425 – 9, 1994, https://doi.org/10.1117/12.198629.

35. Casalicchio, M. L., G. Perrone and A. Vallan, "A fiber optic sensor for displacement and acceleration measurements in vibration tests", *2009 IEEE Instrumentation and Measurement Technology Conference*, pp. 1676–1680, May 2009.

36. Ochsner, J. L., "Minimally Invasive Surgical Procedures", *The Ochsner Journal*, Vol. 2, No. 3, pp. 135–136, 2000,

37. Goldberg, S., "Radiofrequency tumor ablation: principles and techniques", *European Journal of Ultrasound*, Vol. 13, No. 2, pp. 129 – 147, 2001, http://www.sciencedirect.com/science/article/pii/S0929826601001264.

38. Rigby, J. H. and S. B. Dye, "Effectiveness of Various Cryotherapy Systems at Decreasing Ankle Skin Temperatures and Applying Compression", *International Journal of Athletic Therapy and Training*, Vol. 22, No. 6, pp. 32–39, 2017, https://doi.org/10.1123/ijatt.2016-0079.

39. Simon, C. J., D. E. Dupuy and W. W. Mayo-Smith, "Microwave Ablation: Principles and Applications", *RadioGraphics*, Vol. 25, No. suppl_1, pp. S69–S83, 2005, https://doi.org/10.1148/rg.25si055501, pMID: 16227498.

40. Poeggel, S., G. Leen, K. Bremer and E. Lewis, "Miniature Optical fiber combined pressure and temperature sensor for medical applications", *SENSORS, 2012 IEEE*, pp. 1–4, October 2012.

41. Jagannathan, J., N. T. Sanghvi, L. A. Crum, C.-P. Yen, R. Medel, A. S. Dumont, J. P. Sheehan, L. Steiner, F. Jolesz and N. F. Kassell, "High Inten-

sity Focused Ultrasound Surgery of the Brainpart 1-A Historical Perspective with Modern Applications", *Neurosurgery*, Vol. 64, No. 2, pp. 201–211, 2009, http://dx.doi.org/10.1227/01.NEU.0000336766.18197.8E.

42. Schena, E., D. Tosi, P. Saccomandi, E. Lewis and T. Kim, "Correction: Schena, E.; et al. Fiber Optic Sensors for Temperature Monitoring during Thermal Treatments: an Overview. Sensors 2016, 16, 1144", *Sensors*, Vol. 18, No. 4, 2018, http://www.mdpi.com/1424-8220/18/4/1226.

43. Hu, J., H. Huang, M. Bai, T. Zhan, Z. Yang, Y. Yu and B. Qu, "A high sensitive fiber-optic strain sensor with tunable temperature sensitivity for temperature-compensation measurement", *Scientific Reports*, Vol. 7, p. 42430, 2017.

44. Gøthgen, I. H., O. Siggaard-Andersen, J. P. Rasmussen, P. D. Wimberley and N. Fogh-Andersen, "Fiber-optic chemical sensors (Gas-Stat®) for blood gas monitoring during hypothermic extracorporeal circulation", *Scandinavian Journal of Clinical and Laboratory Investigation*, Vol. 47, No. sup188, p. 27–29, 1987.

45. Schlosser, W. F. and R. H. Munnings, "Thermistors as Temperature Sensors at 4.2 K and the Effect of a Magnetic Field", *Review of Scientific Instruments*, Vol. 40, No. 10, pp. 1359–1360, 1969, https://doi.org/10.1063/1.1683796.

46. Plewes, D. B. and W. Kucharczyk, "Physics of MRI: A primer", *Journal of Magnetic Resonance Imaging*, Vol. 35, No. 5, pp. 1038–1054, https://onlinelibrary.wiley.com/doi/abs/10.1002/jmri.23642.

47. Purcell, E. M., H. C. Torrey and R. V. Pound, "Resonance Absorption by Nuclear Magnetic Moments in a Solid", *Phys. Rev.*, Vol. 69, pp. 37–38, January 1946, https://link.aps.org/doi/10.1103/PhysRev.69.37.

48. Bloch, F., "Nuclear Induction", *Phys. Rev.*, Vol. 70, pp. 460–474, October 1946, https://link.aps.org/doi/10.1103/PhysRev.70.460.

49. Jha, S., P. K. Sharma and R. Malviya, "Hyperthermia: Role and Risk Factor for Cancer Treatment", *Achievements in the Life Sciences*, Vol. 10, No. 2, pp. 161 – 167, 2016, http://www.sciencedirect.com/science/article/pii/S2078152016300724.

50. Beppu, T., T. Masuda, T. Ishiko, H. Hayashi, S. Sugiyama, K. Doi, H. Takamori, K. Kanemitsu, M. Hirota and H. Baba, "Radio-frequency ablation (RFA) is equivalent in therapeutic effect but safer compared to microwave coagulation therapy (MCT) for hepatocellular carcinoma", *Journal of Clinical Oncology*, Vol. 25, No. 18_suppl, pp. 15064–15064, 2007, http://ascopubs.org/doi/abs/10.1200/jco.2007.25.18.

51. Hamid Alemohammad, R. L., Amir Azhari, "Fiber optic sensors for distributed monitoring of soil and groundwater during in-situ thermal remediation", *Proc.SPIE*, Vol. 10208, pp. 10208 – 10208 – 6, 2017, https://doi.org/10.1117/12.2270033.

52. Maurer, R. D., "Glass fibers for optical communications", *Proceedings of the IEEE*, Vol. 61, No. 4, pp. 452–462, April 1973.

53. Polishuk, P., "Plastic optical fibers branch out", *IEEE Communications Magazine*, Vol. 44, No. 9, p. 140–148, 2006.

54. Giallorenzi, T. G., "Optical communications research and technology: Fiber optics", *Proceedings of the IEEE*, Vol. 66, No. 7, pp. 744–780, July 1978.

55. Farid, E. and D. Nikolay, "Novel V shaped negative temperature coefficient of conductivity thermistors and electromagnetic interference shielding effectiveness from butyl rubber loaded boron carbide ceramic composites", *Journal of Applied Polymer Science*, Vol. 91, No. 5, pp. 2756–2770, https://onlinelibrary.wiley.com/doi/abs/10.1002/app.13458.

56. Kwakernaak, A., J. Hofstede, J. Poulis and R. Benedictus, "Improvements in

bonding metals (steel, aluminium)", *Advances in Structural Adhesive Bonding*, p. 185–236, 2010.

57. Sun, B., D.-R. Kong, S.-W. Li, D.-F. Yu, G.-J. Wang, F.-F. Yu, Q. Wu and J.-M. Xu, "Validation of an Endoscopic Fibre-Optic Pressure Sensor for Noninvasive Measurement of Variceal Pressure", *BioMed Research International*, Vol. 2016, p. 1–7, 2016.

58. Noh, Y., S. Sareh, H. Würdemann, H. Liu, J. Back, J. Housden, K. Rhode and K. Althoefer, "Three-Axis Fiber-Optic Body Force Sensor for Flexible Manipulators", *IEEE Sensors Journal*, Vol. 16, No. 6, pp. 1641–1651, March 2016.

59. Giallorenzi, T. G., J. A. Bucaro, A. Dandridge and J. H. Cole, "Optical-fiber sensors challenge the competition: Resistance to corrosion and immunity to interference head the list of benefits in detecting stimuli ranging from pressure to magnetism", *IEEE Spectrum*, Vol. 23, No. 9, pp. 44–50, September 1986.

60. Sze, S., *Semiconductor devices, physics and technology*, 1985, `https://books.google.com.tr/books?id=gb0QAQAAMAAJ`.

61. Akinlami, J. O. and A. O. Ashamu, "Optical properties of GaAs", *Journal of Semiconductors*, Vol. 34, No. 3, p. 032002, 2013, `http://stacks.iop.org/1674-4926/34/i=3/a=032002`.

62. Goldschmidt, V. M., "Crystal structure and chemical constitution", *Trans. Faraday Soc.*, Vol. 25, pp. 253–283, 1929, `http://dx.doi.org/10.1039/TF9292500253`.

63. Frese, K. W., "Simple method for estimating energy levels of solids", *Journal of Vacuum Science and Technology*, Vol. 16, No. 4, pp. 1042–1044, 1979, `https://doi.org/10.1116/1.570159`.

64. Nag, B., "Direct band-gap energy of semiconductors", *Infrared Physics Technology*, Vol. 36, No. 5, pp. 831 – 835, 1995,

http://www.sciencedirect.com/science/article/pii/135044959500023R.

65. Richard, S., F. Aniel and G. Fishman, "Energy Band Structure Of Si, Ge And GaAs Over The Whole Brillouin Zone Via The k.p Method", *AIP Conference Proceedings*, Vol. 772, No. 1, pp. 1123–1124, 2005, https://aip.scitation.org/doi/abs/10.1063/1.1994504.

66. Cepheiden, *Deutsch: einfaches Banddiagramm von GaAs (nur 1. Valenz- und Leitungsband)*, June 2006.

67. Varshni, Y., "Temperature dependence of the energy gap in semiconductors", *Physica*, Vol. 34, No. 1, pp. 149 – 154, 1967, http://www.sciencedirect.com/science/article/pii/0031891467900626.

68. Sahu, P. C. and N. V. C. Shekar, "Pressure induced phase transition behaviour in f-electron based dialuminides", *Pramana*, Vol. 54, No. 5, p. 685–708, 2000.

69. Dow, J. D. and D. Redfield, "Toward a Unified Theory of Urbach's Rule and Exponential Absorption Edges", *Phys. Rev. B*, Vol. 5, pp. 594–610, January 1972, https://link.aps.org/doi/10.1103/PhysRevB.5.594.

70. Swinehart, D. F., "The Beer-Lambert Law", *Journal of Chemical Education*, Vol. 39, No. 7, p. 333, 1962, https://doi.org/10.1021/ed039p333.

71. Geng, P., W. Li, X. Zhang, X. Zhang, Y. Deng and H. Kou, "A novel theoretical model for the temperature dependence of band gap energy in semiconductors", *Journal of Physics D: Applied Physics*, Vol. 50, No. 40, p. 40LT02, 2017, http://stacks.iop.org/0022-3727/50/i=40/a=40LT02.

72. Zoroofchi, J. and J. K. Butler, "Refractive index of n type gallium arsenide", *Journal of Applied Physics*, Vol. 44, No. 8, pp. 3697–3699, 1973, https://doi.org/10.1063/1.1662823.

73. Hung, K. Y., P. H. Wu, T. W. Tsai, D. C. Shye and H. c. Wu, "Application of Fresnel equations to improve interface reflection of inclined exposure and develop micro-mirrors for blu-ray DVDs", *2009 IEEE International Conference on Industrial Technology*, pp. 1–6, February 2009.

74. Honnell, P. M., "A new universal right-hand rule", *Electrical Engineering*, Vol. 72, No. 4, pp. 346–349, April 1953.

75. Petrova-Mayor, A. and S. Gimbal, "Advanced lab on Fresnel equations", *American Journal of Physics*, Vol. 83, No. 11, pp. 935–941, 2015, `https://doi.org/10.1119/1.4929969`.

76. Karlsson, A., "Approximate Boundary Conditions for Thin Structures", *IEEE Transactions on Antennas and Propagation*, Vol. 57, No. 1, pp. 144–148, January 2009.

77. Muhibbullah, M., A. M. A. Haleem and Y. Ikuma, "Frequency dependent power and energy flux density equations of the electromagnetic wave", *Results in Physics*, Vol. 7, pp. 435 – 439, 2017, `http://www.sciencedirect.com/science/article/pii/S2211379716302170`.

78. Bryant, F., "Snell's Law of Refraction", *Physics Bulletin*, Vol. 9, No. 12, p. 317, 1958, `http://stacks.iop.org/0031-9112/9/i=12/a=004`.

79. Grado-Caffaro, M. and M. Grado-Caffaro, "On the wavelength dependence of the refractive index of photons", *Optik - International Journal for Light and Electron Optics*, Vol. 112, No. 5, pp. 221 – 222, 2001, `http://www.sciencedirect.com/science/article/pii/S0030402604700418`.

80. Skauli, T., P. S. Kuo, K. L. Vodopyanov, T. J. Pinguet, O. Levi, L. A. Eyres, J. S. Harris, M. M. Fejer, B. Gerard, L. Becouarn and E. Lallier, "Improved dispersion relations for GaAs and applications to nonlinear optics", *Journal of Applied Physics*, Vol. 94, No. 10, pp. 6447–6455, 2003,

https://doi.org/10.1063/1.1621740.

81. Edlén, B., "The Refractive Index of Air", *Metrologia*, Vol. 2, No. 2, p. 71, 1966, http://stacks.iop.org/0026-1394/2/i=2/a=002.

82. Talghader, J. and J. S. Smith, "Thermal dependence of the refractive index of GaAs and AlAs measured using semiconductor multilayer optical cavities", *Applied Physics Letters*, Vol. 66, No. 3, pp. 335–337, 1995, https://doi.org/10.1063/1.114204.

83. McCullough, L. and S. Arora, "Diagnosis and treatment of hypothermia", *American family physician*, Vol. 70, No. 12, p. 2325—2332, December 2004, http://europepmc.org/abstract/MED/15617296.

84. Sund-Levander, M. and E. Grodzinsky, "Assessment of body temperature measurement options", *British Journal of Nursing*, Vol. 22, No. 16, p. 942–950, 2013.

85. Chicheł, A., J. Skowronek, M. Kubaszewska and M. Kanikowski, "Hyperthermia – description of a method and a review of clinical applications", *Reports of Practical Oncology Radiotherapy*, Vol. 12, No. 5, pp. 267 – 275, 2007, http://www.sciencedirect.com/science/article/pii/S150713671060065X.

86. Mcclelland, G., "Tissue Respiration — Cellular Respiration", *Encyclopedia of Fish Physiology*, p. 951–958, 2011.

87. H., L. E., P. R. A. and R. R. J., "Experimental Thermal Burns, Especially the Moderate Temperature Burn", *Quarterly Journal of Experimental Physiology and Cognate Medical Sciences*, Vol. 32, No. 1, pp. 67–86.

88. Lee, J. T., E. S. Lee, J. K. Won and H. Z. Choi, "Wafer Polishing Process with Signal Analysis and Monitoring for Optimum Condition of Machining", *Advanced Materials Research*, Vol. 126-128, p. 295–304, 2010.

89. Steffanson, M. and I. Rangelow, "Microthermomechanical infrared sensors", *Opto-Electronics Review*, Vol. 22, No. 1, p. 1–15, January 2014.

90. Weilmeier, M. K., K. M. Colbow, T. Tiedje, T. V. Buuren and L. Xu, "A new optical temperature measurement technique for semiconductor substrates in molecular beam epitaxy", *Canadian Journal of Physics*, Vol. 69, No. 3-4, p. 422–426, 1991.

91. Mohammadnejad, S., S. Soleimaninezhad, N. J. Abkenar and A. Bahrami, "Optimized Single and Double Layer Antireflection Coatings for GaAs Solar Cells", *International Journal Of Renewable Energy Research*, Vol. 3, pp. 79 – 83, 2016.